63-3-3

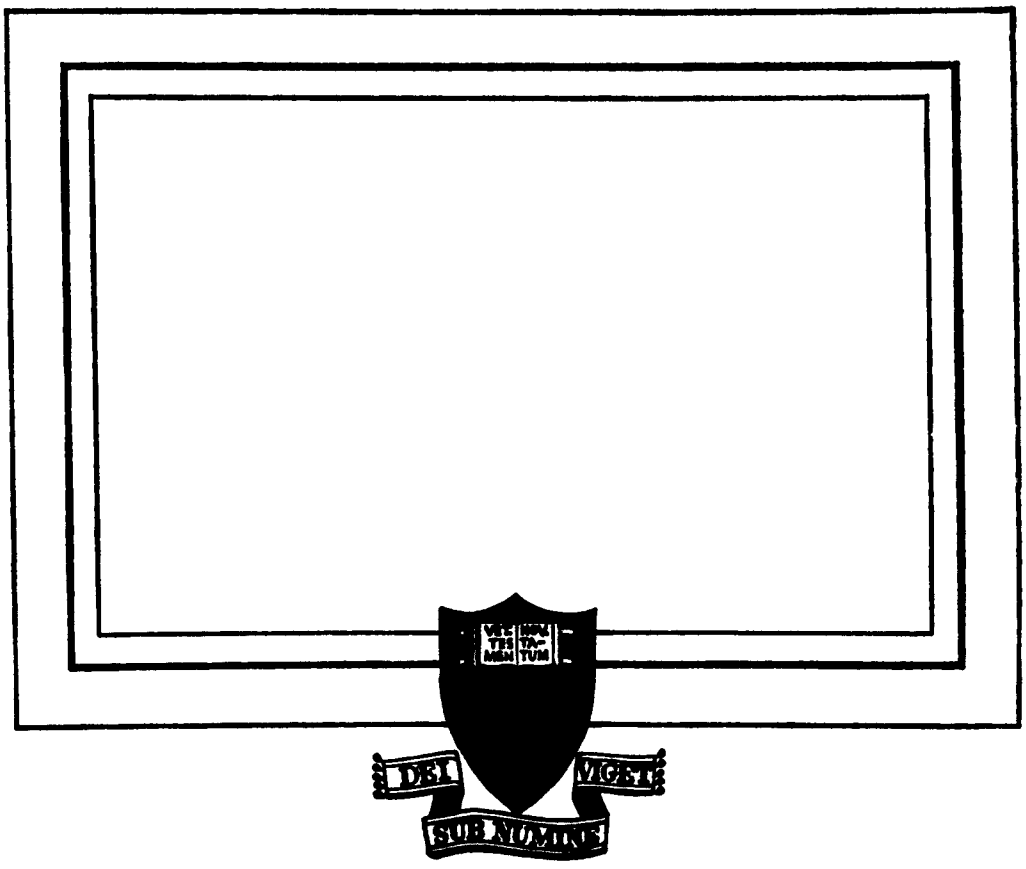

PRINCETON UNIVERSITY
PLASTICS LABORATORY

PLASTICS LABORATORY
TECHNICAL REPORT

No. 67A

PIEZO-RESISTIVE CHARACTERISTICS OF SOME ORGANIC SEMICONDUCTING POLYMERS

A. W. Henry and C. Cappas

April 15, 1963

Contract No. DA-31-124-ARO(D)-21

The work reported here was supported partly by the Army, Navy and Sandia Corporation under Contract No.DA-31-124-ARO(D)-21; ONR 356-375

TABLE OF CONTENTS

ABSTRACT

A series of highly conjugated polymers with semiconducting characteristics, was examined to determine the piezo-resistive behavior. The resistivities ranging from 10^2 to 10^{11} ohm-cm at room temperature and 1840 atmospheres pressure, decreased 100, and for some polymers, 1000 fold as the pressure was increased to 35,000 atmospheres.

Elimination of voids and particle-to-particle contact problems was obtained by the extreme pressures used as evidenced by: (a) absence of hysteresis in the piezo-resistivity, and (b) low measured permeation rate to air.

A correlation between the extrapolated activation energy for the polyacene quinone radical (PAQR) polymers and the number of fused rings in the aromatic portion of the polymer was obtained.

An elemental polymeric semiconductor with high conductivity (i.e. p-type tellurium), was also observed to have a decreasing thermoelectric power with increased pressure and a relatively constant activation energy, both due to the p-type TeO_2 impurity.

Introduction

This work attempts to correlate the observed piezo-resistive changes of various organic semiconducting-polymers. It is a continuation of earlier work started at the Plastics Laboratory during 1961[1].

Other work has been done concerning the piezo-resistive effect of various metallic semiconductors. Balchan and Drickamer[2] reported that selenium exhibits a rapid drop in resistance between 60 and 128 kilobars pressure, with the material suddenly dropping to the resistance of a metal at 128 kilobars, due probably to a sudden rearrangement of the atomic structure at this pressure.

Ioffe[3], reported that tellurium also showed a drop in resistance with increased pressure.

Experimental

Materials

The polymer 6AWH was prepared by reacting pyrene, pyromellitic anhydride, and $ZnCl_2$ catalyst in a 1-1/2 mole ratio respectively, at 306°C.[4,9] The other PAQR polymers used, (i.e. the EHE series) were prepared by Engelhardt, himself.[4,9] He also prepared the Schiff's base polymer, 106 EHE.[4,9]

Apparatus

The apparatus, as shown in Figure 1, consisted of two braced Bridgman-type tungsten-carbide anvils of about 0.2 inch diameter faces. The anvils were surrounded by stainless-steel

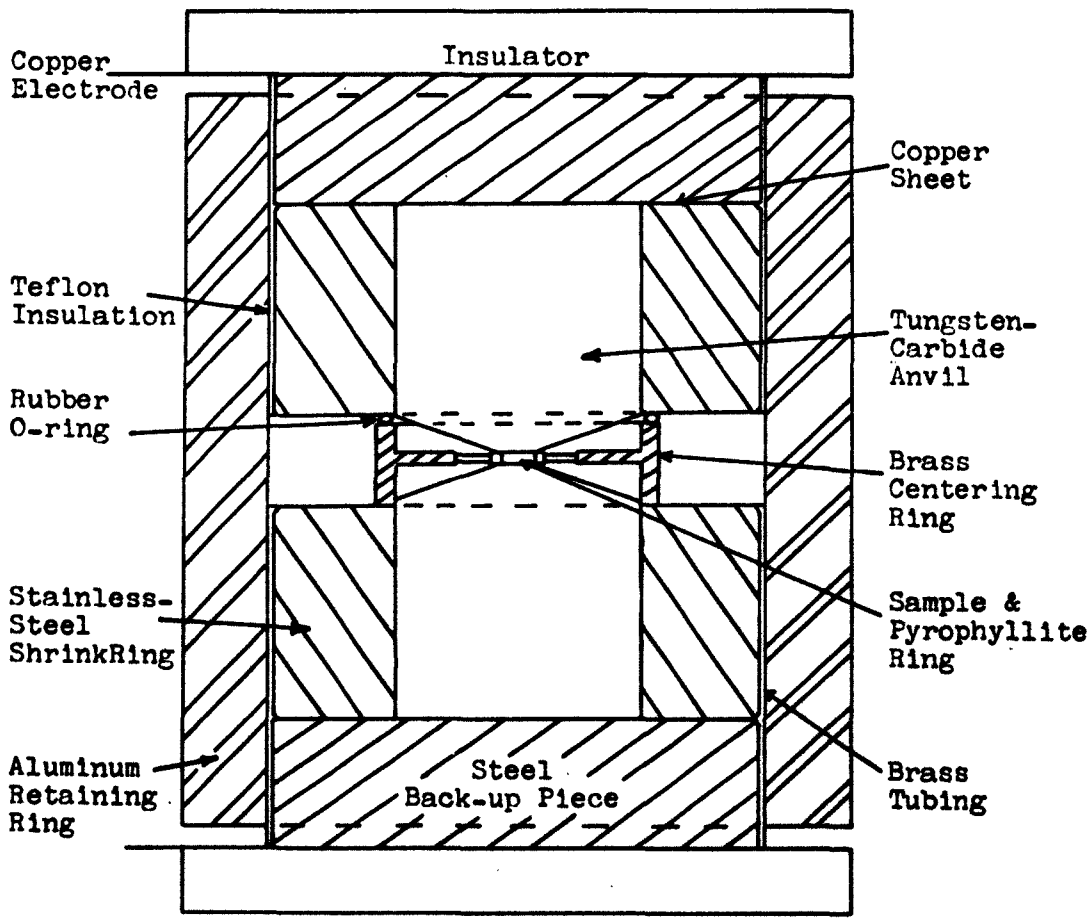

Figure 1, Anvil apparatus used to make the resistance versus $(\text{Load})^{\frac{1}{2}}$ runs on the PAQR polymers.

shrink rings to help neutralize some of the compressive stresses. Surrounding the bottom anvil was a brass centering collar, which rested on the stainless-steel shrink ring of the bottom anvil. A soft rubber O-ring was placed on the top of the collar to prevent the top anvil from making electrical contact with the bottom one.

The actual sample of material, a polyacene quinone radical polymer synthesized by Engelhardt,[4,9] for example, was finely ground and dried for at least 200 hours in a desiccator before testing. The sample was then tamped inside a pyrophyllite ring whose inside diameter was just slightly larger than 0.2 inches and about 70 mils thick. It was discovered later that a thinner ring, (i.e. 10-20 mils), coated with ferric oxide, better prevented the sample from being squeezed out between the anvil faces, which occasionally caused the anvils to slip and crack against each other. This lateral slip process was generally not observed with the anvil set-up as shown in Figure 1, but only with anvils which were poorly aligned. The anvil set-up shown in Figure 1, was well aligned, because of a paper disk which fitted snugly around the pyrophyllite disk and into the brass collar; and also due to the tightly-fitting aluminum shielding ring which surrounded both anvils and steel back-up pieces. The top anvil was insulated by a piece of thin Teflon sheet which completely surrounded the upper shrink ring and back-up piece. Copper sheet, 5 mils thick, was placed between the anvils and their back-up pieces to afford a more uniform distribution of pressure.

The whole assembly was placed inside an aluminum box to further shield the cell electrically. It was insulated from the press by two 3/8 inch thick phenolic blocks.

A 610A Keithley Electrometer was used to measure the resistance of the cell via electrically shielded leads.

The cell was placed in a Watson-Stillman press of 50 tons maximum force, and which could theoretically exert a maximum pressure of about 175,000 atmospheres on the 0.2 inch diameter anvil faces.

The samples were run at the maximum pressure and temperature first to obtain a thoroughly compacted sample for the subsequent temperature and pressure runs.

The resistances were recorded only as the pressure was increased to the particular pressure levels because of the hysteresis exhibited by the press itself, due to piston drag as the pressure was released, as shown in Figure 2. The load was reproducible to within a few percent as long as the resistances were recorded on the way up, as can be seen from the graphs of resistance versus $(\text{load})^{1/2}$, Figures 4-6. These figures are representative of all the runs made with the various polymers. The hysteresis deflection calibration-curve was obtained by using a thick piece of steel with four strain gages attached as shown in Figure 3(a), and connected in a Wheatstone bridge arrangement, Figure 3(b).

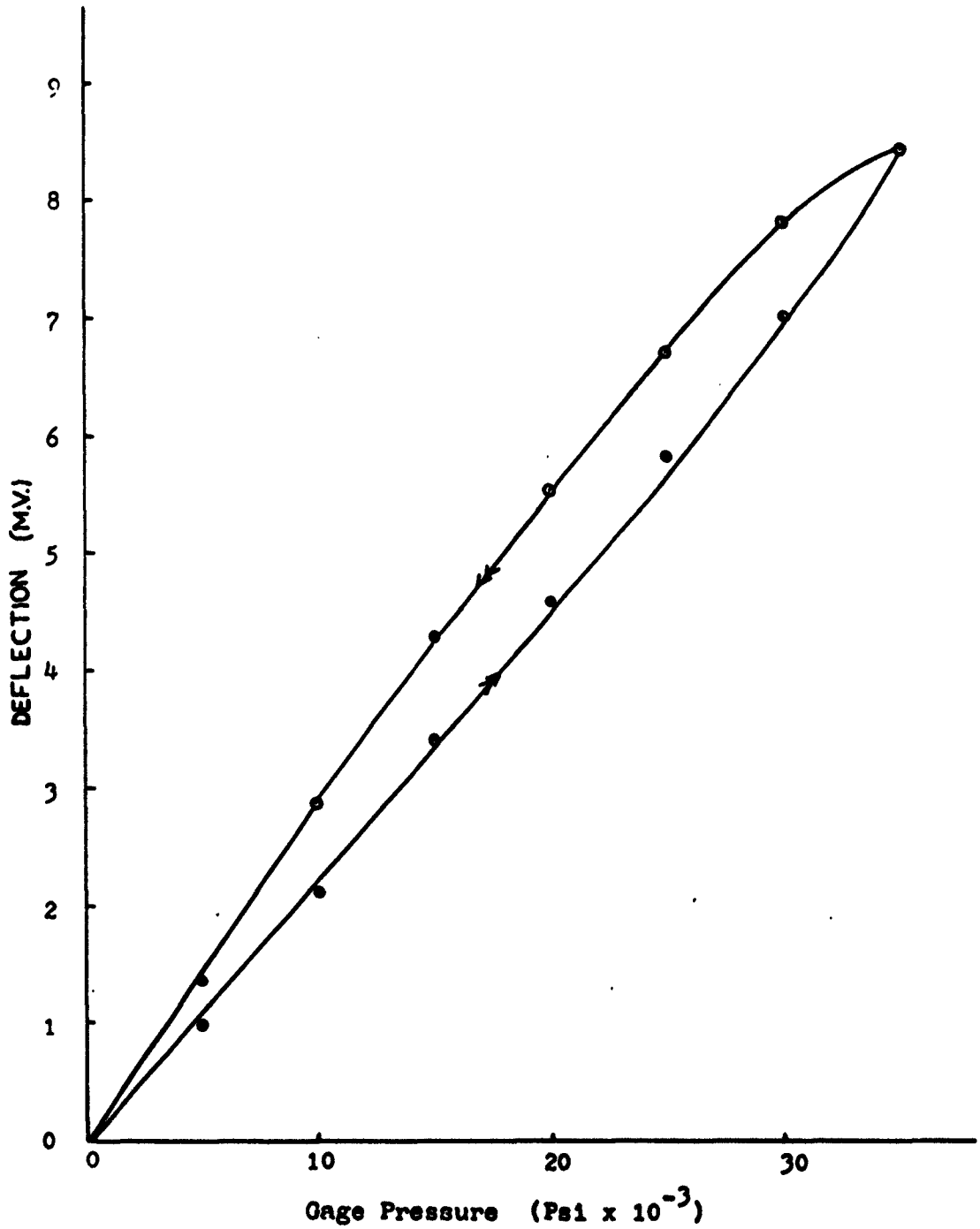

Figure 2, Hysteresis plot: deflection of steel versus the Gage pressure.

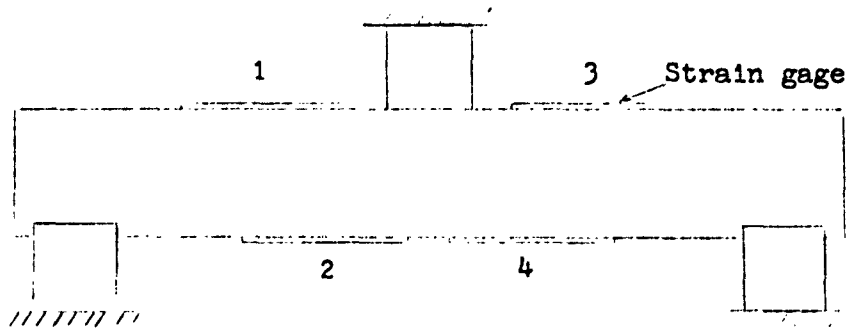

Figure 3(a), Strain gage arrangement on the steel bar.

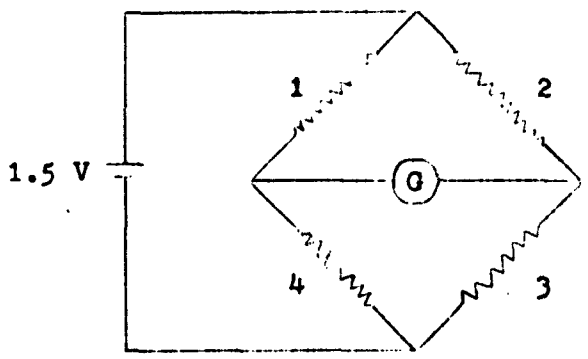

Figure 3(b), Wheatstone bridge arrangement of the strain gages to measure deflections of the bar.

Results and Discussion of PAQR Runs

An homologous series of PAQR polymers was examined. The acene part of the polymer varied, as shown in Table I, from napthalene to dibenzpyrene. The quinone part of the polymer was obtained by using pyromellitic anhydride. From the graphs, Figures 4-6, a good correlation between resistance and $(\text{load})^{1/2}$ or in fact $(\text{pressure})^{1/2}$, can be seen for various temperatures[1].

Using the equation: $\sigma = \sigma_o e^{-E_a/kT}$

where σ = conductivity at temperature T

σ_o = a constant

k = Boltzman constant

E_a = activiation energy

one can calculate the activation energy of the polymers at various increasing pressures. Figures 7 and 8, illustrate that there is also a good correlation between the activation energy of the polymers and the load or pressure on the material. E_a decreases with increased $(\text{pressure})^{1/2}$. This is in agreement with theory[1].

A similar expression can be derived for the change in the area of contact between the PAQR polymer molecules as the pressure is increased.[1] This change in area represents a change in entropy[1], and as such should be independent of temperature and may be expected to be about the same for each polymer in the homologous series. Table I, shows that the entropy-pressure coefficient, b", is indeed relatively insensitive to the temperature; and that the values for b" are fairly similar over the

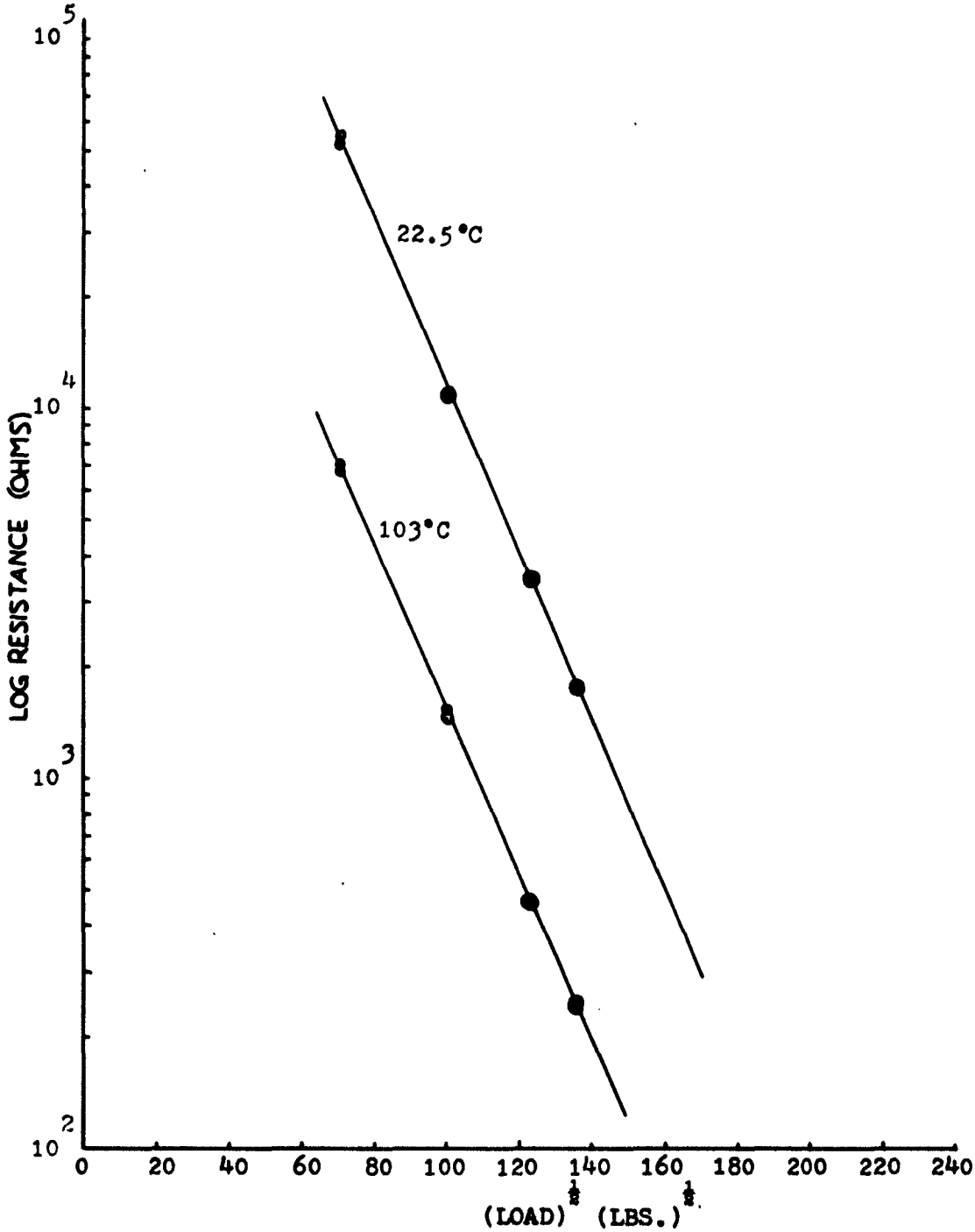

Figure 4, Log of resistance versus the $(\text{Load})^{\frac{1}{2}}$ for polymer 53 EHE.

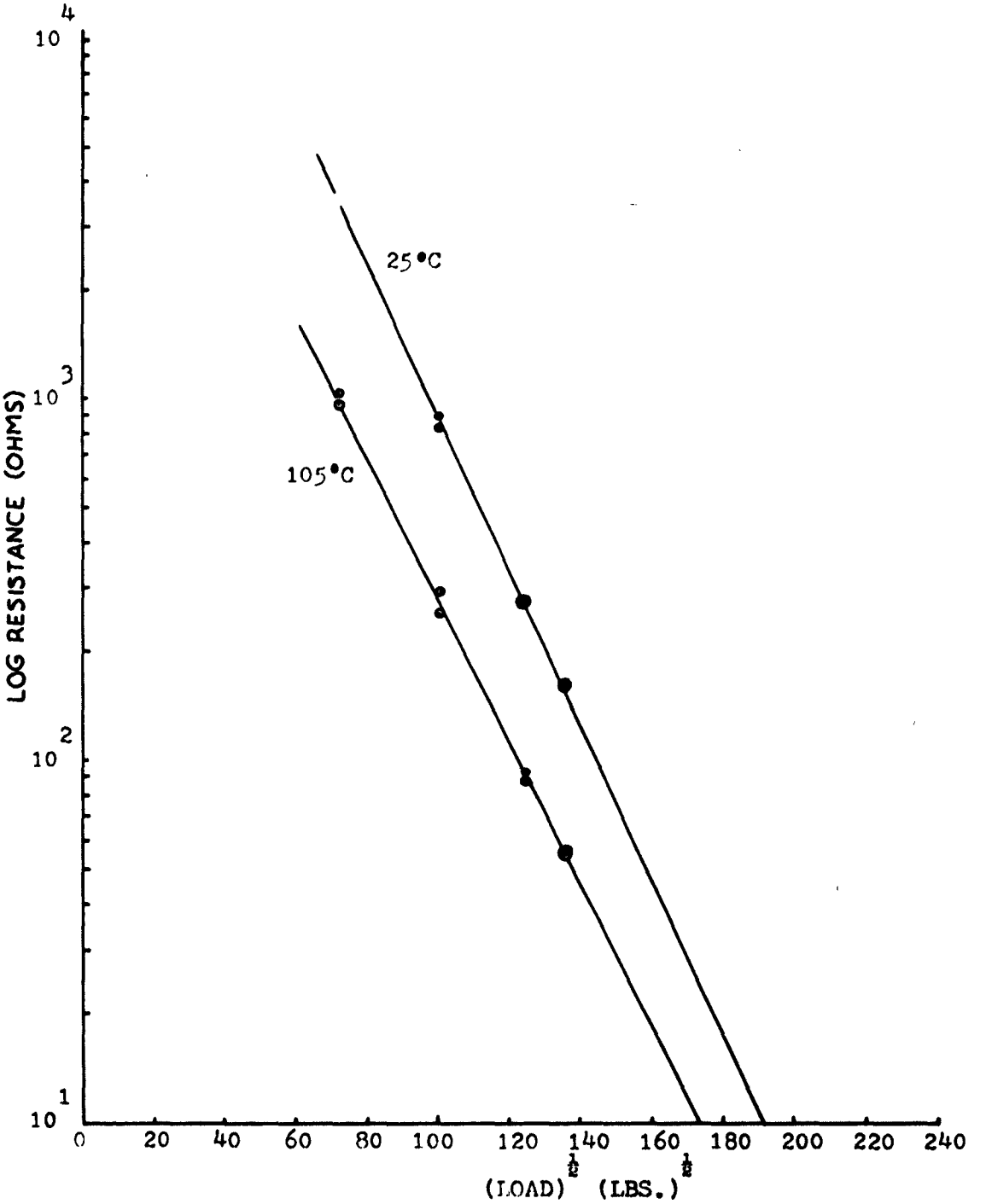

Figure 5, Log of resistance versus the $(\text{Load})^{\frac{1}{2}}$ for polymer 6 AWH

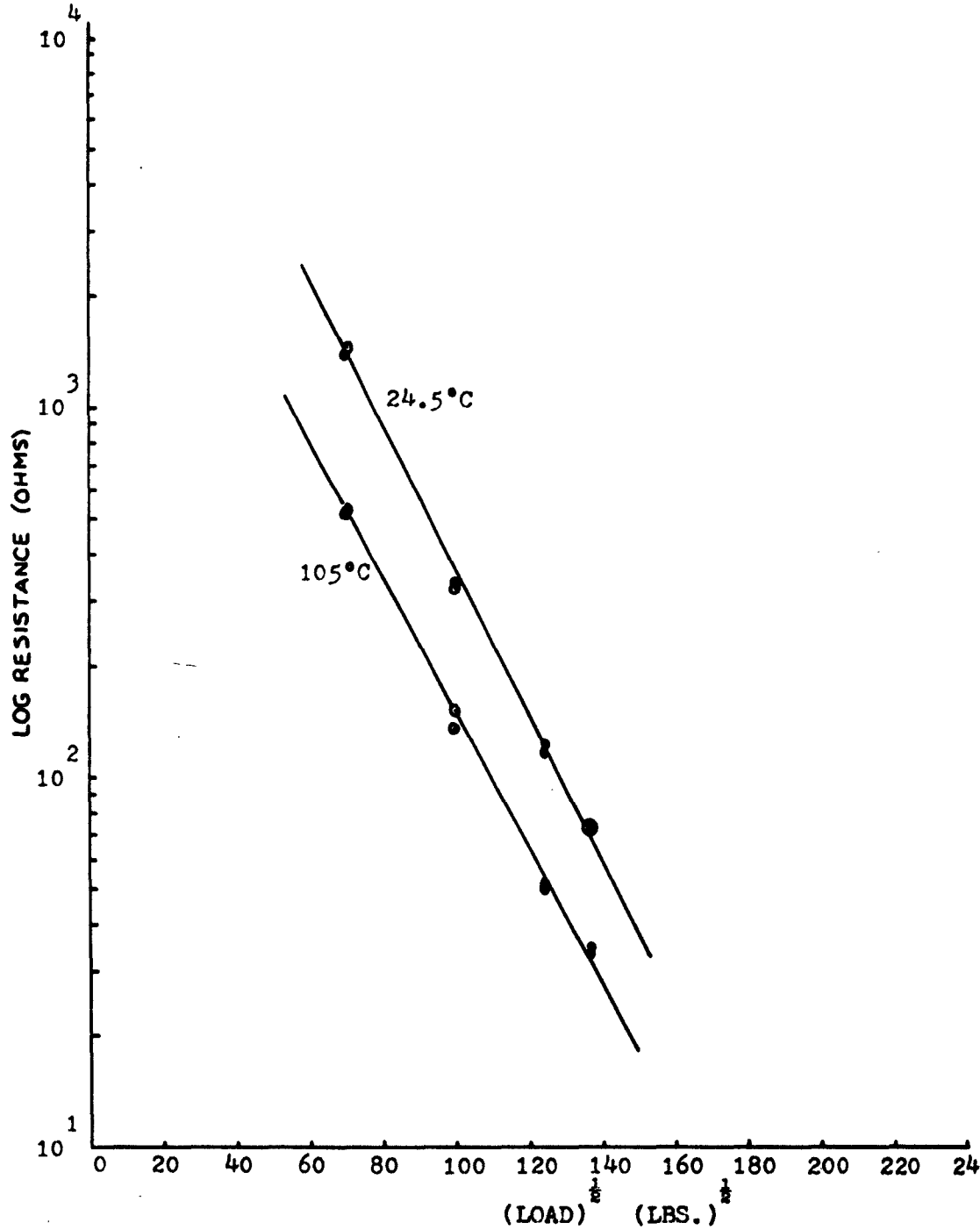

Figure 6, Log resistance versus the $(\text{Load})^{\frac{1}{2}}$ for polymer 85 EHE

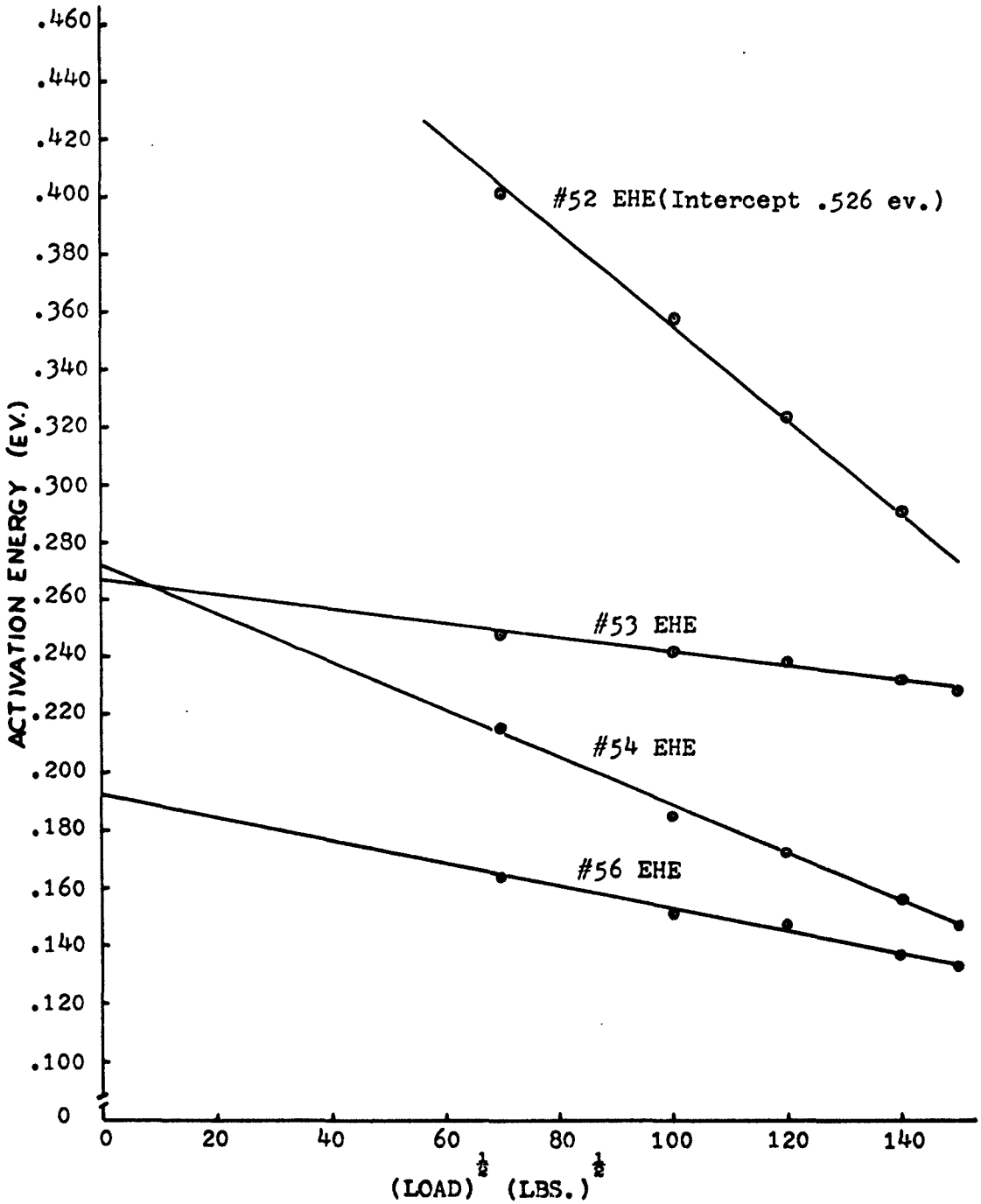

Figure 7, Activation energy versus the $(\text{Load})^{\frac{1}{2}}$ for the PAQR polymers numbered above.

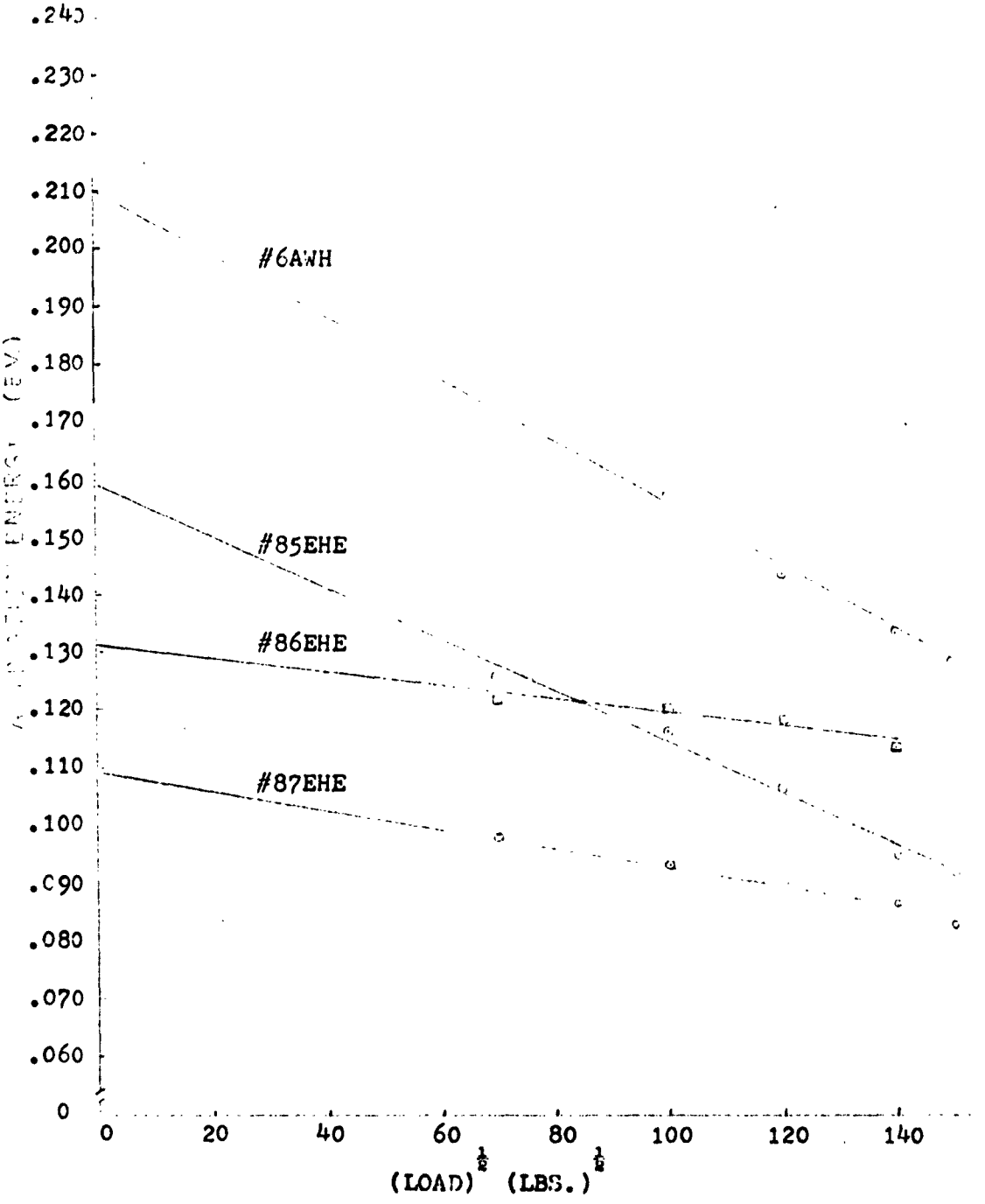

Figure 8, Activation energy versus the $(\text{Load})^{\frac{1}{2}}$ for the PAQR polymers numbered above.

TABLE I

Pressure-Conductivity Parameters for Various Semiconducting Polymers

Sample No.	Composition	T°C	Entropy-Pressure Coef $b'' \times 10^6$ eV/(atm)$^{1/2}$ (°K)	Activ. Energy Pressure Coef $b_o \times 10^3$ eV/(atm)$^{1/2}$ (°K)	E_{a_o} (eV)
51EHE	Terphenyl-PMA	25	0.180	1.055	0.410
		105	0.220	1.055	0.410
52EHE	Napthalene-PMA	23	0.990	1.235	0.526
		107	1.000	1.235	0.526
53EHE	Anthracene-PMA	22	2.836	0.187	0.267
		103	2.733	0.187	0.267
54EHE	Phenanthrene-PMA	30	1.420	0.636	0.2725
		112	1.420	0.636	0.2725
6AWH	Pyrene-PMA	25	1.830	0.415	0.210
		105	1.835	0.415	0.210
56EHE	Chrysene-PMA	29	2.340	0.314	0.1935
		98	2.355	0.314	0.1935
85EHE	Perylene-PMA	25	1.825	0.347	0.1595
		105	1.840	0.347	0.1595
86EHE	Dibenzpyrene-PMA	27	2.385	0.0916	0.131
		105	2.448	0.0916	0.131
87EHE	Picene-PMA	29	2.655	0.1285	0.1095
		113	2.657	0.1285	0.1095
106EHE	1,4 Napthaquinone TODI	23	-8.000	3.140	1.000
		99	-7.800	3.140	1.000

Note: PMA = Pyromellitic anhydride
TODI = p-toluene diisocyanate

entire series. The activation energy plus a constant shown in Table I, was obtained by extrapolating the activation energy versus $(load)^{1/2}$ plot, Figures 7 and 8, to zero pressure.[1] At low pressures, the constant "c" becomes comparable to the activation energy-pressure coefficient, b_o,[1] times the $(pressure)^{1/2}$, i.e. $(c > b_o P^{1/2}$ in the equation: $E = E_o + c - (c^2 + b_o{}^2 P)^{1/2})$, and hence "c" can not be neglected. The extrapolated activation energy does show a drop as the acene part of the polymer increases in the number of fused rings and becomes more highly conjugated as can be noted in Table I. The more highly conjugated the molecules, the easier it is for an electron or hole to traverse it. Eley[8] has reported that the change in energy levels or width of energy gaps is inversely proportional to the number of π-electrons, hence to the number of fused rings. This theory exhibits a good correlation for the PAQR polymer series. Figure 9.

The activation energy-pressure coefficient, "b_o", was obtained by taking the slope of the activation energy versus the $(load)^{1/2}$ plot, i.e. from Figures 7 and 8. The values of "b_o" for the various polymers in the series could not be correlated to the degree of conjugation, or number of fused aromatic rings in the acene part of the polymer. However, there is a good correlation between E_{a_o} and b_o as is to be expected, (see Figure 9 (a)), for the higher the energy barrier the more easily it will be reduced by an increase in pressure.

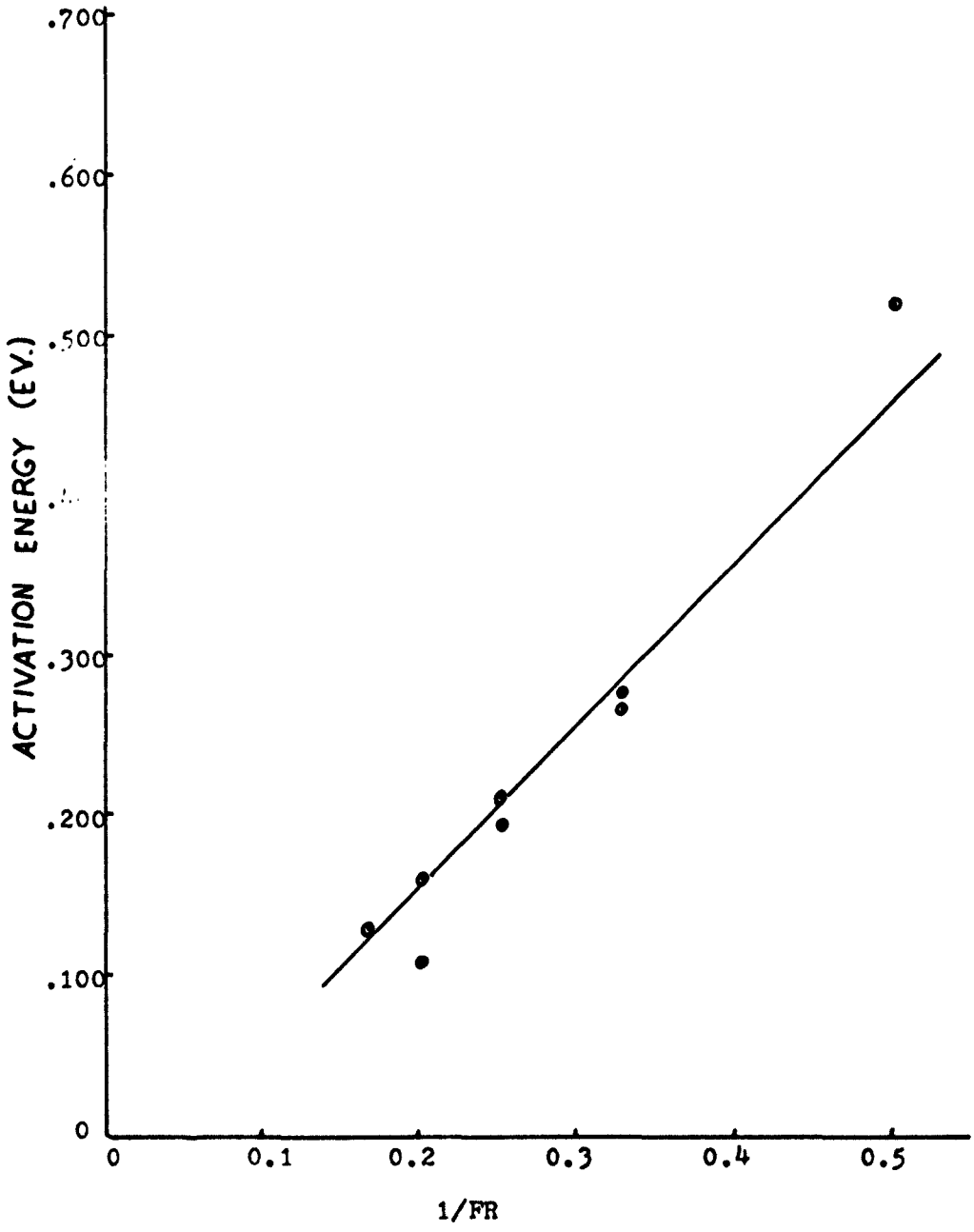

Figure 9 The extrapolated activation energy of the PAQR polymers versus one over the No. of fused rings in the Acene part of the polymers.

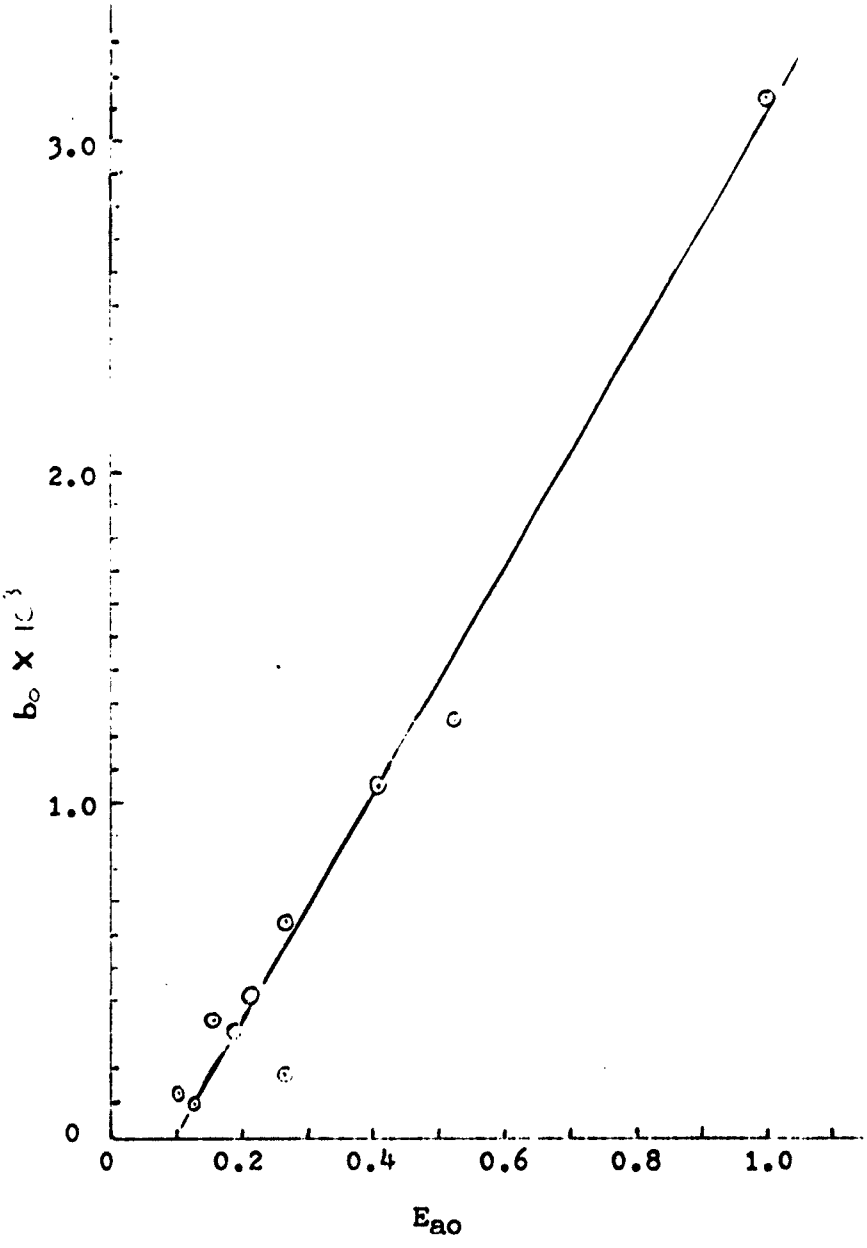

Figure 9(a) The activation energy-pressure, b_o, coefficient versus the extrapolated activation energy.

Permeation of Samples

The purpose of this experiment was to find out whether the PAQR polymers would compress to a homogeneous, non-porous disk or remain a porous agglomeration of powder particles. If the sample had remained porous, the reduction in resistance with increased pressure could be interpreted as due partly to particle-particle contacting, rather than due principally to having the molecules themselves being pushed more closely together by the increased pressure.

The apparatus consisted of a vacuum pump, a McLeod vacuum gage, a three-way stopcock, and glass and rubber tubing arranged as shown in Figure 10. The system was evacuated without the sample to obtain a reference leak rate. The sample, sealed against a coarse porous glass filter with rubber cement, was then included in the system and the leak rate redetermined. The permeability calculation is shown in the appendix.

The sample tested, a representative material of the homologous PAQR series, exhibited a permeation coefficient of less than $8 \times 10^{-8} \frac{cc/sec\text{-}cm}{cm^2\text{-}atm}$ which shows it to be fairly impermeable. For comparison, helium has a permeation coefficient through Mylar film of 1×10^{-6} (in same units).

This low permeation rate for the PAQR sample proved that the samples were compacted to non-porous disks under the conditions of the experiment. It also substantiates the postulation that the piezo-resistive effect observed was due to molecule-

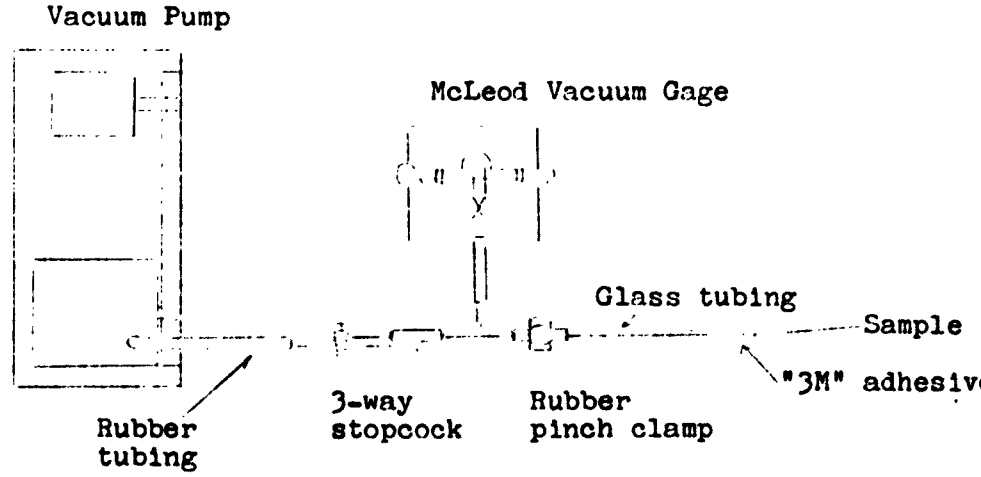

Figure 10, The permeation apparatus.

molecule approach, and to an increase in orbital overlap between molecules, causing an overall decrease in activation energy for the hopping of electrons or holes from one molecule to another. This is also confirmed by the lack of hysteresis in the pressure-resistance curves.

Molecular Complexes

Aromatic hydrocarbons by themselves have relatively high resistivities: 10^{12} to 10^{18} ohm-cm. However, recently Kommandeur and Hall[5], reported that a molecular complex of an aromatic hydrocarbon, (e.g. perylene or pyrene), and iodine would, when prepared in the proper stoichiometric ratio, have a conductivity 10 to 12 orders of magnitude higher. They proved that it was pure electronic and not ionic conductivity, by passing 10,000 times the amount of current through the sample needed to decompose it according to Faraday's laws, but observed no change in the conductivity.

The conductivity in this type of complex is particularly interesting for the bonding between the iodine and the aromatic hydrocarbon is of the dative covalent type. The materials form a sort of infinite sandwich-type molecular complex, i.e. alternate layers of aromatic and iodine molecules stacked one on top of the other.

The pyrene.2 iodine complex was prepared according to Kommandeur and Hall[5]. The complex is stable at room temperature only if kept under its own vapor pressure, hence it was stored in a desiccator containing excess iodine crystals.

The complex showed a decrease in resistance with (pressure) 1/2 the range in resistivities being from about 650 ohm-cm at 7000 atmospheres pressure to about 510 ohm-cm at 35,000 atmospheres, see Figure 12. Since the structurally soft complex was pressure sensitive, and was an ideal model of polymer molecules being squeezed closer and closer together, it can be concluded that the piezo-resistive changes being observed in the covalently bonded macromolecules were due to a closer approach of the molecules with an overall decrease in the hopping and carrier formation activation energy.

Metallic Runs

By referring again to Figures 4-8, it can be seen that possibly the polymers could reach practically zero resistance or zero activation energy if the pressure were raised high enough. It can also be thought of in molecular terms, that the molecules on being pushed closer and closer together, would have lowered the hopping barriers between them. In the limit, there would be no distinction between the molecules (i.e. like a metal), and an electron or hole would be free to move easily and instantaneously throughout the system.

With this in mind, an attempt was made to attain "metallic" character in a few of the most conductive polymers on hand. Some of the runs were made using the high pressure equipment at the Signal Corps Testing Center at Fort Monmouth, New Jersey, with the valuable assistance of Dr. A. Giardini.

The tungsten-carbide anvils used there had 1/2 inch diameter faces. These anvils, as shown in Figure 11, were unsupported, i.e. they did not have a shrink-fitted ring around them. The press was calibrated as to pressure developed between the anvils. The force was controlled by a valve in an automatically pumped oil system.

The highest pressure reached with the unsupported anvils was 98,000 atmospheres. This pressure, as can be seen from Figure 12, was still not quite high enough to cause the polymers tested to go "metallic". In this particular series of runs, the polymers were not subjected to a pre-compaction at high temperature and pressure before recording the piezo-resistive changes. The greater curvature of the plots in this instance is undoubtedly due in large measure to this.[4,9]

The polymers definitely did show the tendency to approach metallic conduction, but one can not be more specific since a pressure higher than 98,000 atmospheres was not attainable.

The samples were surrounded by thin pyrophyllite rings, coated with ferric oxide. The attainment of these low resistances was not due to the anvils touching on the periphery of the samples, since the smallest sample thickness, which was measured at the end of the run, was 14 mils. The tungsten-carbide anvils had been ground flat by diamond lapping them, using a Hyprez diamond compound of a 15-30 micron grade.

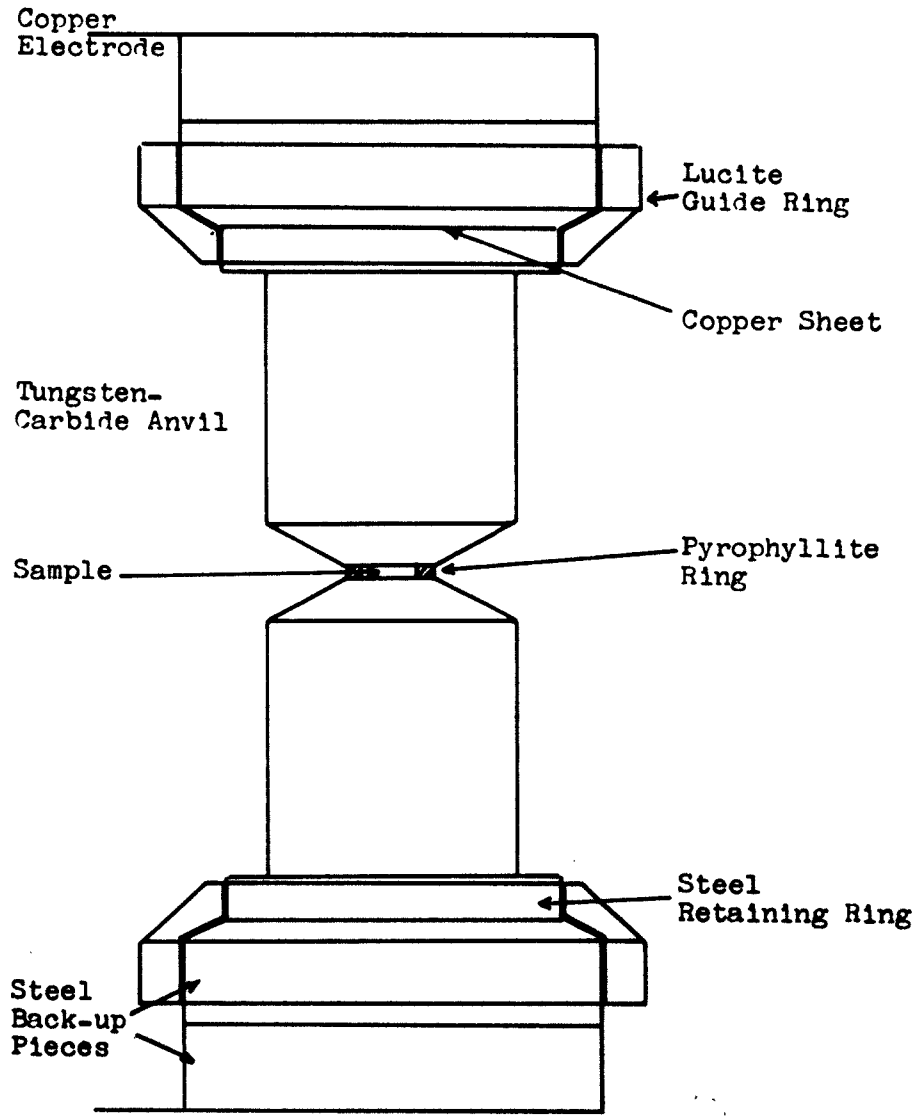

Figure 11, Anvil apparatus used at Fort Monmouth, New Jersey

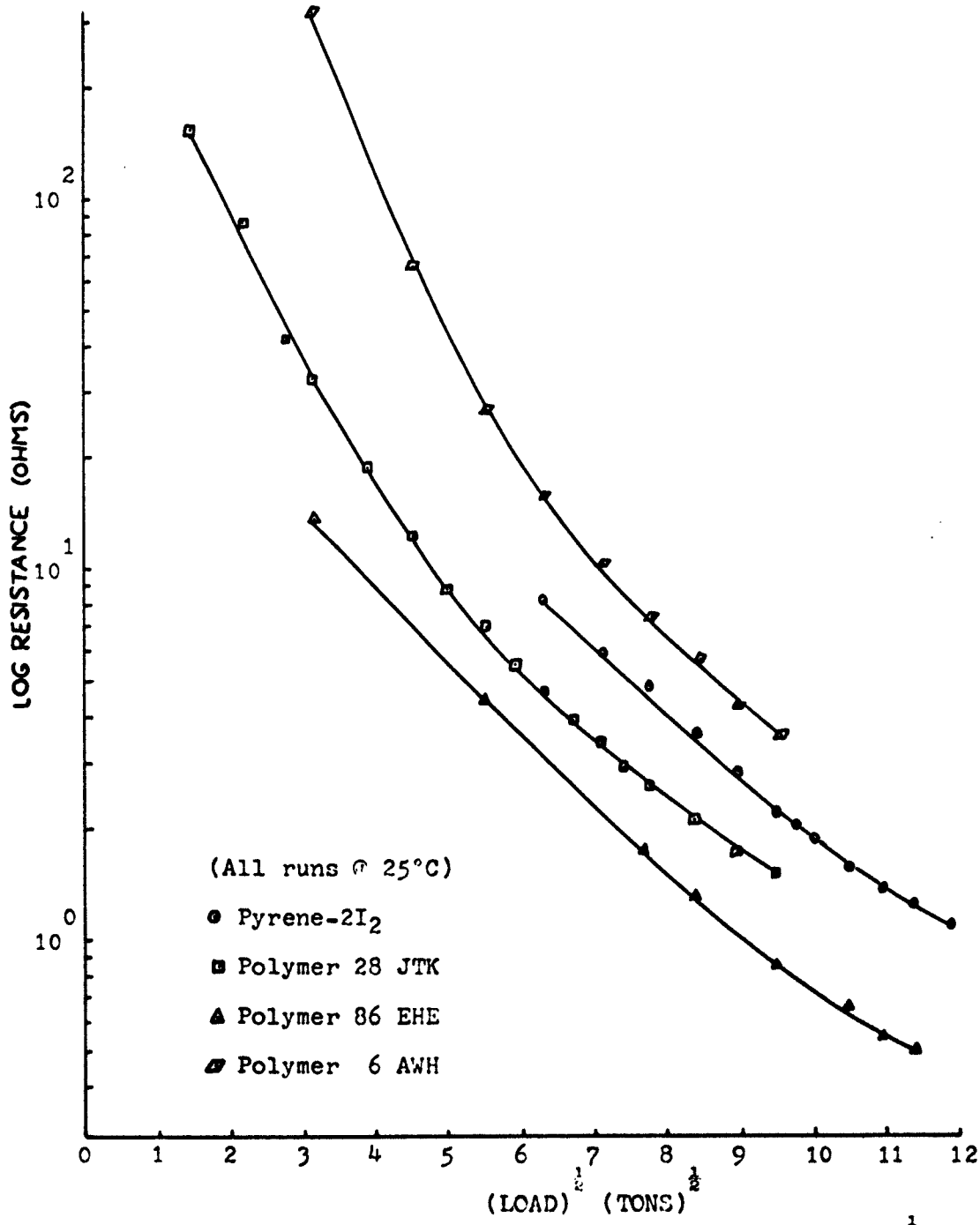

Figure 12, Log of resistance versus $(Load)^{\frac{1}{2}}$ for polymers listed above. Runs made at Fort Monmouth, N.J.

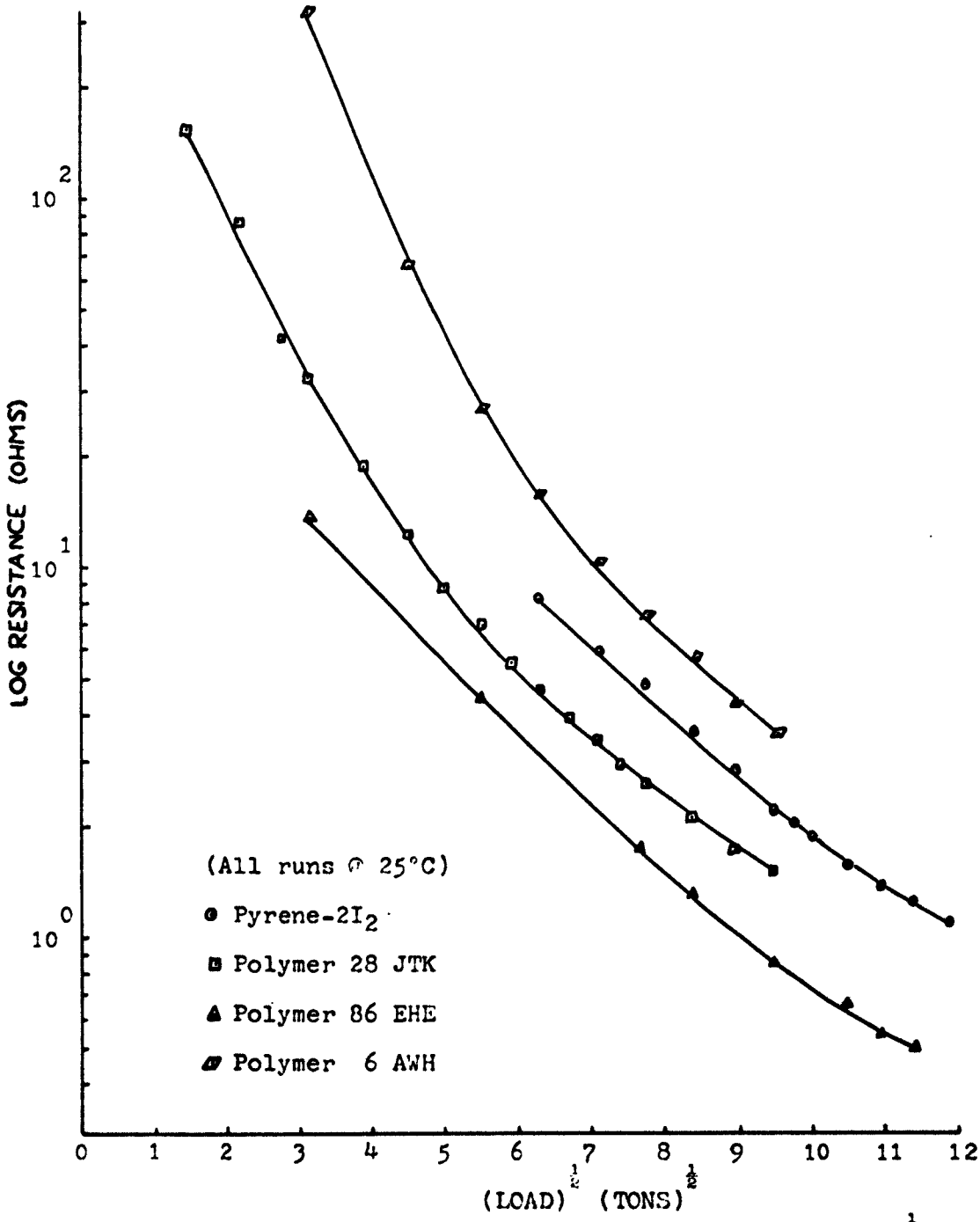

Figure 12, Log of resistance versus $(Load)^{\frac{1}{2}}$ for polymers listed above. Runs made at Fort Monmouth, N.J.

Other Organic Polymers

A Schiff's base type polymer, 106 EHE, i.e. 1,4-napthaquinone and p-toluene diisocyanate in a (1:1) mole ratio was tried. It showed a straight line correlation between resistance and $(\text{load})^{1/2}$, just as the PAQR polymers had, see Figure 13. However, its extrapolated activation energy at zero pressure was much higher than that of the PAQR polymers, "E_{a_o} + c" being about 1.00 eV compared to the PAQR range of from 0.1095 to 0.526 eV. The activation energy-pressure coefficient was also higher by a factor of almost three times that of the highest "b_o" for a PAQR polymer; the latter being 1.235×10^{-3} and the former 3.14×10^{-3}. The entropy-pressure coefficient was different by about a factor of four and was minus in sign: -8×10^{-6}, cf. Table I for comparison. It would seem that the mechanism for conduction in the PAQR polymers is different from that in Schiff's base type polymers.

Polytetrachlorothiophenol and a polymer 28 JTK, made from a (1:1) mole ratio of pyromellitic anhydride and chloroacetic acid using $ZnCL_2$ as catalyst, both showed the usual straight line correlation between $(\text{load})^{1/2}$ and resistance, see Figures 14 and 15. However, neither of these polymers showed a variation in activation energy with pressure; it remained fairly constant at about 0.15 eV. It is believed therefore, that the decrease in resistance was caused mainly by an increase in mobility of the carriers.

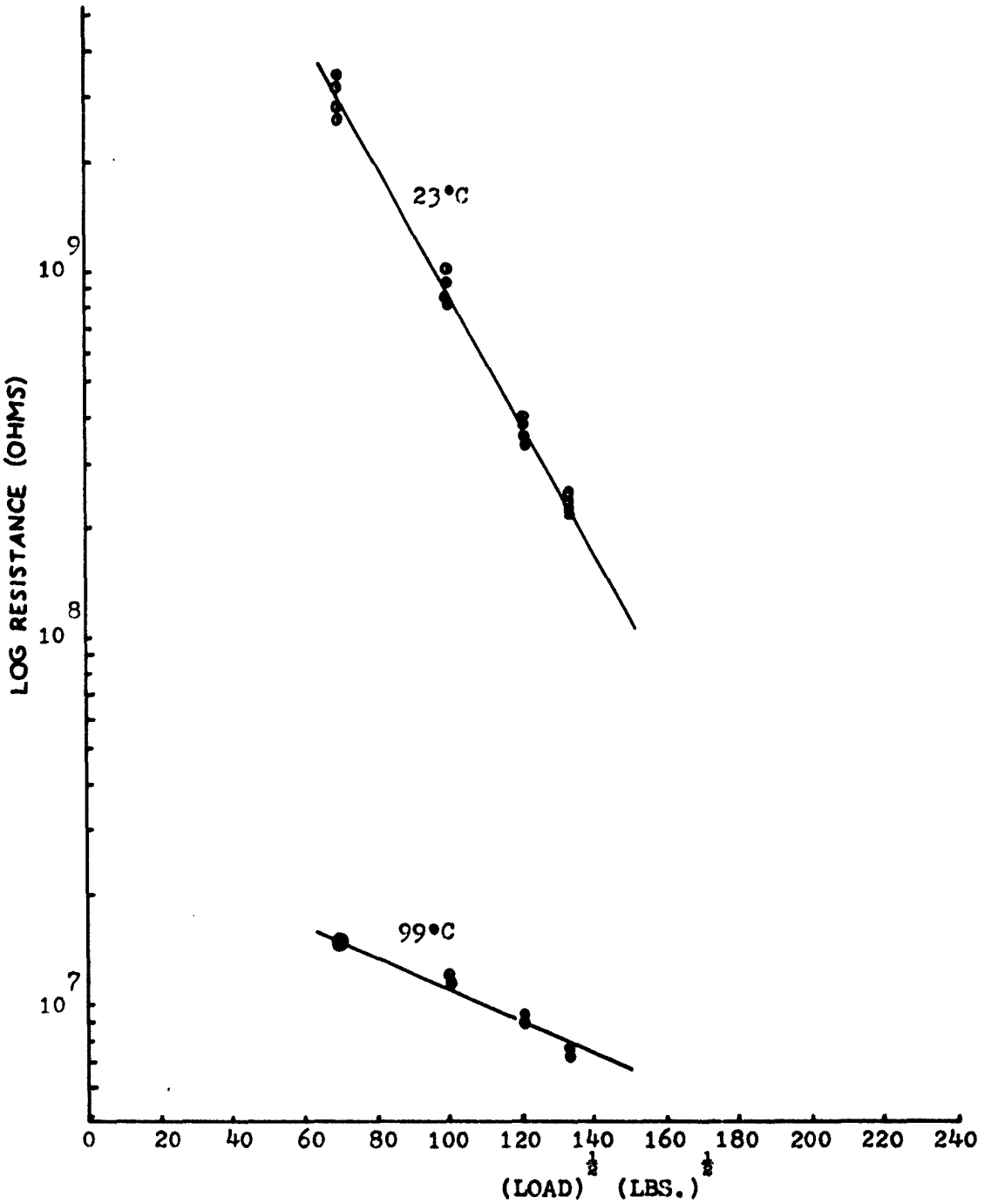

Figure 13, Log of resistance versus the $(\text{Load})^{\frac{1}{2}}$ for polymer 106 EHE

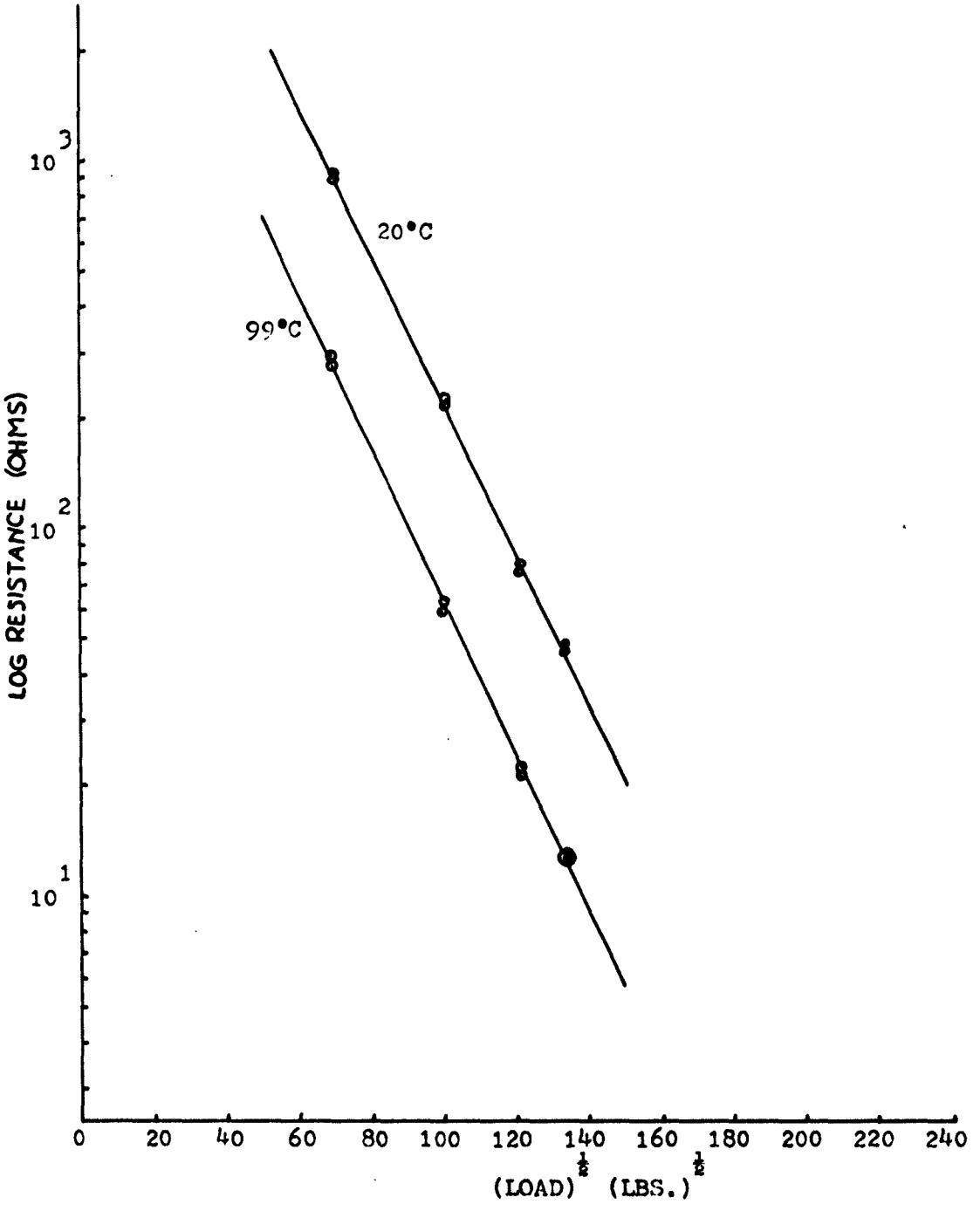

Figure 14, Log resistance versus the $(Load)^{\frac{1}{2}}$ for Polytetrachlorothiophenol

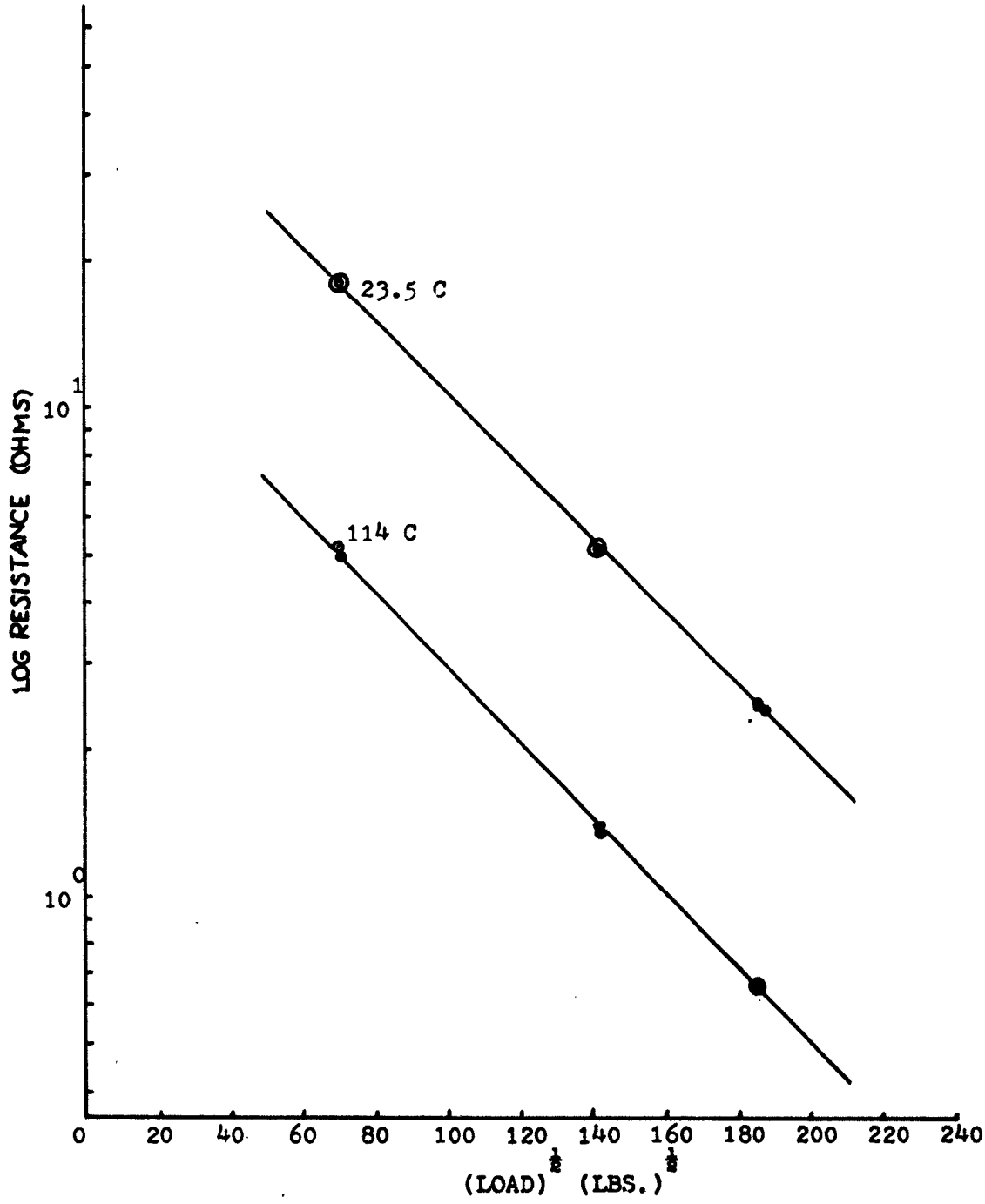

Figure 15, Log of resistance versus the $(\text{Load})^{\frac{1}{2}}$ for polymer 28 JTK

Figure of Merit - FOM

An important consideration in determining the feasibility of the polymers tested for use in pressure sensing devices, is their Figure of Merit. It can be defined as the signal to noise ratio in a typical circuit. A sample calculation for the FOM of a common strain gage and one of the semiconducting polymers can be found in the appendix. FOM values for the polymers as well as their room temperature resistivities determined at or extrapolated to 1840 atmospheres, are listed in Table II. As a reference the FOM for a common strain gage is about 0.4×10^{-3}. The values listed for the polymers show considerably higher FOM's than the strain gage, and thus are interesting as potentail materials in pressure sensing devices.

Tellurium

Ioffe[3] reported pressure runs with tellurium showing a decrease of the original energy gap of the material, (i.e. 0.34 eV) with pressure, until at about 30,000 atmospheres, the tellurium attained zero energy gap or became metallic.

It appeared desirable to re-examine this energy gap versus pressure correlation for p-type tellurium. Since the actual resistance of the tellurium sample was small, i.e. around 10^{-2} ohms, the resistance was measured using a constant current passed through the sample, and by determining the voltage across the sample by a 150A Keithley Microvolt-Ammeter as the pressure was varied. The corrected resistance versus $(\text{load})^{1/2}$ plot is shown by Figure 16. The resistance was corrected for the varying resistance of

TABLE II

Figure of Merit and Room Temperature Resistivities of the Polymers Tested

Sample No.	Composition	F.O.M.	Resistivity (ohm-cm)
51 EHE	Terphenyl-PMA	1.49×10^{-3}	1.05×10^{8}
52 EHE	Napthalene-PMA	1.22×10^{-3}	1.48×10^{7}
53 EHE	Anthracene-PMA	1.53×10^{-3}	3.32×10^{6}
54 EHE	Phenanthrene-PMA	1.58×10^{-3}	3.59×10^{6}
6 AWH	Pyrene-PMA	1.63×10^{-3}	3.82×10^{5}
56 EHE	Chrysene-PMA	1.59×10^{-3}	1.00×10^{6}
85 EHE	Perylene-PMA	1.74×10^{-3}	1.25×10^{5}
86 EHE	Dibenzpyrene-PMA	2.02×10^{-3}	2.10×10^{4}
87 EHE	Picene-PMA	1.93×10^{-3}	2.35×10^{5}
106 EHE	1,4-Napthaquinone-TODI	1.35×10^{-3}	1.19×10^{11}
28 JTK	Chloroacetic acid_PMA	1.55×10^{-3}	4.00×10^{2}
	Polytetrachlorothiophenol	1.68×10^{-3}	3.38×10^{6}

NOTE: PMA = Pyromellitic anhydride
TODI = p-toluenediisocyanate

the cell itself with pressure, and for the thermal emf's generated by the various connections in the system.

The effective energy gap of the p-type tellurium sample remained constant to within experimental error, at about 0.125 eV over the entire range of pressure, (i.e. from 3500 to 18,000 atmospheres). Ioffe[3] had reported (presumably for intrinsic tellurium) that under hydrostatic pressure, the energy gap drops to 0.20 eV at 11,000 atmospheres, to 0.1 eV at 17,000 atmospheres and to zero at 30,000 atmospheres.

The p-type tellurium examined here, showed a flattening-out of resistance versus $(\text{load})^{1/2}$, see Figure 16, at about 18,000 atmospheres, (i.e. at 180 $\text{lbs.}^{1/2}$ on the graph). It seems logical to believe that this smaller impurity energy gap (0.125 eV) would dominate until the pressure reached 18,000 atmospheres. At this point, the intrinsic energy gap of the pure tellurium is about 0.1 eV[3], and hence the decreased energy gap of the pure tellurium would start to compete with the impurity level in supplying carriers. From that point on, as the pressure increases, the conductivity of the material would be controlled mainly by the then smaller energy gap of the intrinsic tellurium.

The Seebeck coefficient of the material was determined to see if a change in Q could be seen as the pressure was increased, and to determine the type and concentration of impurity. The low-pressure Seebeck apparatus, Figure 17, consisted of two platinum-coated aluminum pieces, between which the sample was placed. A Teflon gasket and brass back-ring helped hold the sample in

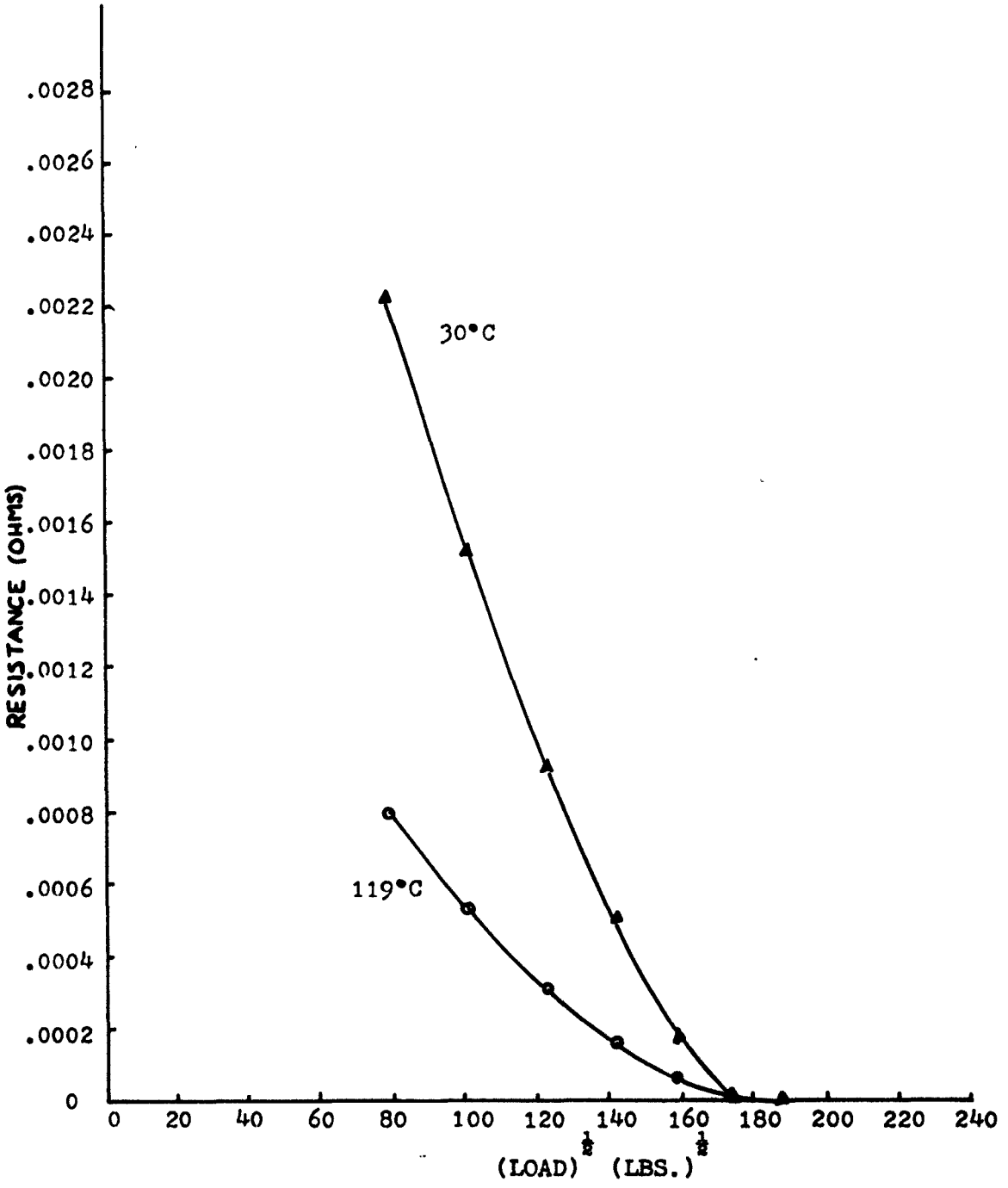

Figure 16, Corrected resistance versus (Load)$^{\frac{1}{2}}$ for Tellurium

place, as well as guide the top and bottom aluminum pieces together. The top block was heated electrically to obtain temperature gradient across the sample. Two thermometers, readable to a tenth of a degree, were used to determine the ΔT across the sample. The voltage produced by the thermal gradient was recorded on a 150A Keithley Microvolt-Ammeter. The maximum pressure attainable with this apparatus, 210 atmospheres, was not high enough to show any drop in Q due to the increased pressure. The Q value obtained at these low pressures was $+ 282\ \mu V/^{\circ}C$.

The Seebeck coefficient was obtained at higher pressures by using the apparatus for the pressure versus resistance runs on the p-type tellurium. The temperature difference across the sample was measured using a pyrometer for each pressure interval, and the voltage produced was recorded by a 150A Keithley Microvolt-Ammeter. The result of this thermoelectric power versus pressure run is shown in Figure 18, and shows a definite dependence of the thermoelectric power on the pressure, it decreases with an increase in pressure. A possible explanation of this, is that the thermoelectric power would also be controlled initially by the large population of impurity carriers, hence giving a relatively large voltage due to a slight temperature gradient ($0.10^{\circ}C$) in the pressure cell, see Figure 19. As the pressure increased the number of intrinsic carriers becomes appreciable, until again competition occurred between the intrinsic and impurity carriers. This competition would cut the

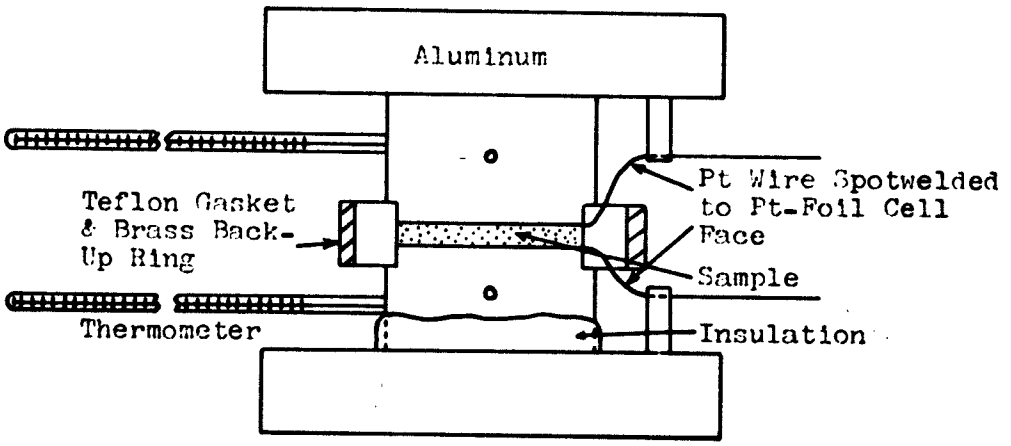

Figure 17, Apparatus for measuring the Seebeck Coefficient.

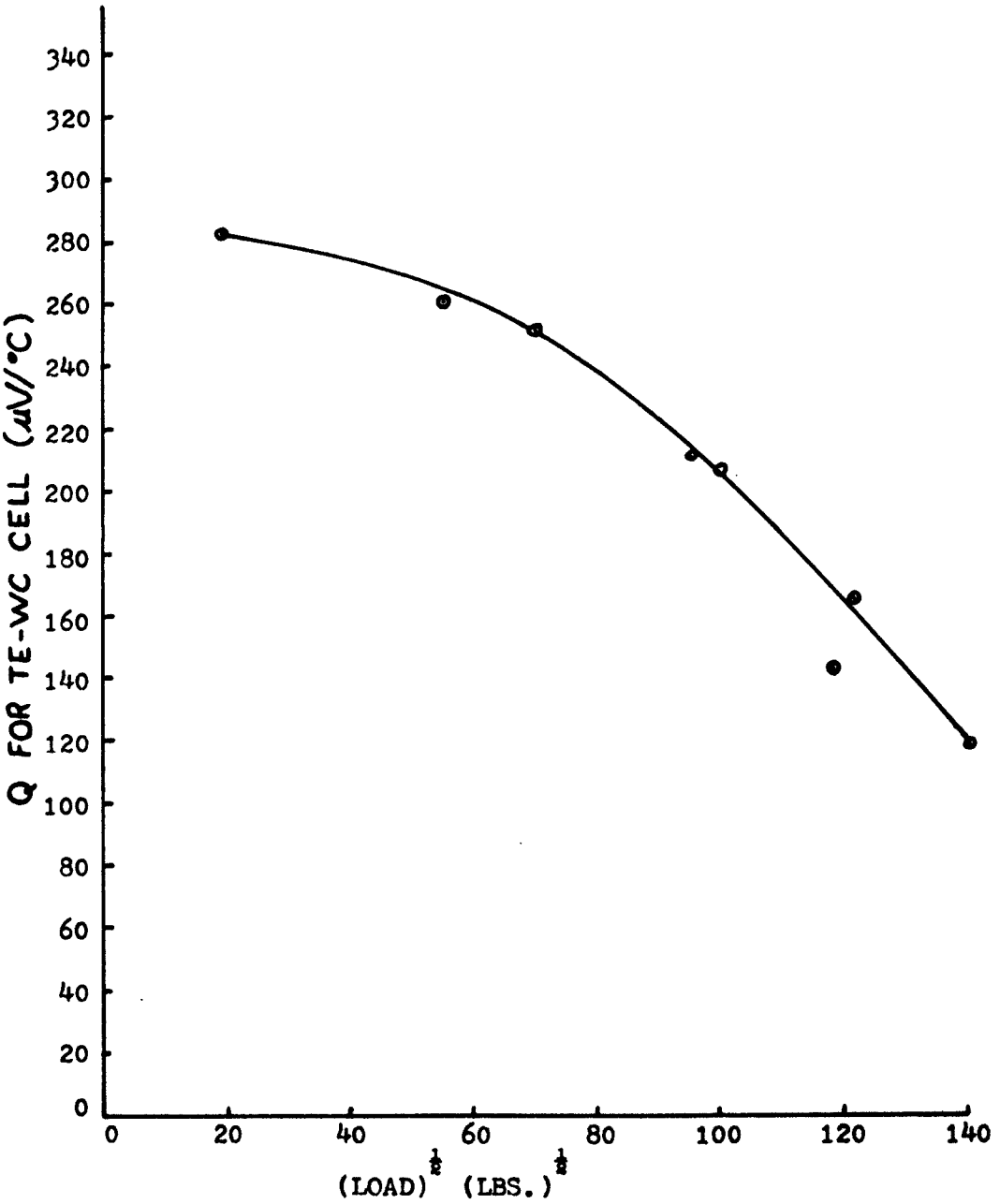

Figure 18, The thermoelectric power coefficient of the tellurium-tungsten carbide cell versus the $(\text{Load})^{\frac{1}{2}}$.

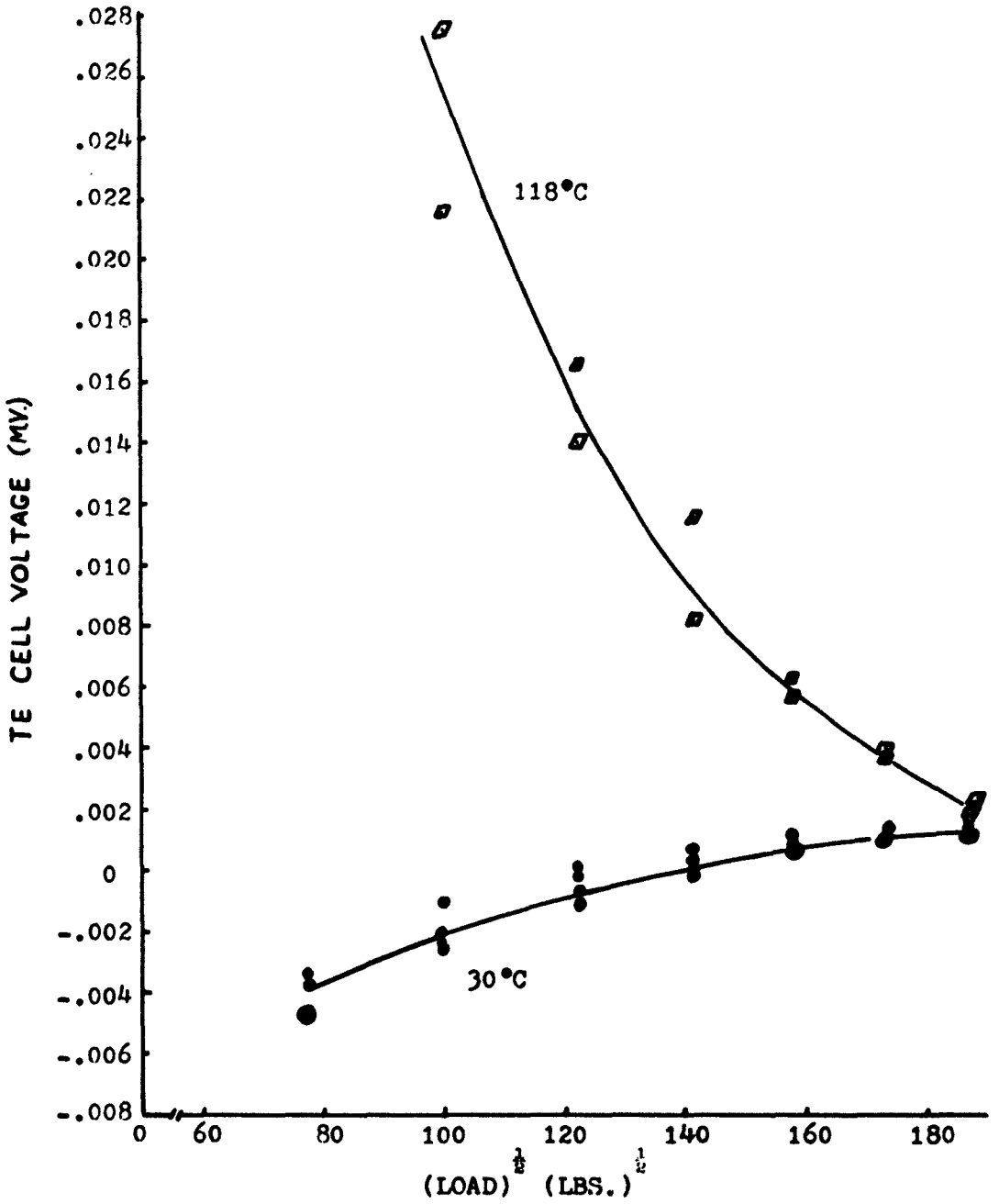

Figure 19, The Tellurium cell voltage versus the $(Load)^{\frac{1}{2}}$.

voltage, Figure 19, because usually the Q impurity and Q intrinsic are of opposite sign[6]; the Q intrinsic becoming larger as the pressure neared 18,000 atmospheres and the energy gap of the pure tellurium approached the impurity energy gap of 0.125 eV. Q total = Q intrinsic + Q impurity[6]

This observation of a transition from extrinsic conduction, due to the impurity energy gap, to intrinsic behavior by the application of pressure, is similar to the transition from extrinsic to intrinsic behavior of semiconductors by increasing the temperature.

An interesting paper by Horne[7] on tellurium gives confirmation to these postulations made about the sample of tellurium tested here. Horne stated that TeO_2 is present in most tellurium samples unless they are doubly or even triply vacuum distilled. TeO_2 has a large effect on the thermoelectric power of the material, (i.e. the higher the TeO_2 content, the higher the thermoelectric power). Triply distilled tellurium gives a value of -160 $\mu V/^{\circ}C$, and the oxide saturated tellurium gives a value of +390 $\mu V/^{\circ}C$. He also noted that the TeO_2 did act as a p-type impurity in tellurium as was observed here in the Seebeck run (+282 $\mu V/^{\circ}C$). Since this tellurium sample gave such a high positive Q, it is probable that it was almost saturated with TeO_2. This is further confirmed by the observed constancy in energy gap of the material up to 18,000 atmospheres, due to this p-type impurity.

Conclusions

1. There is a definite correlation between the resistance of certain of the organic semiconducting polymers and the pressure to which they are subjected.

2. In the PAQR polymers, the range of activation energies is from about 0.1 to 0.5 eV; and the range of resistivities is from about 10^4 to 10^8 ohm-cm at low pressure.

3. The activation energies and resistivities of the PAQR polymers are functions of the number of fused aromatic rings in the acene part of the polymer.

4. The entropy-pressure coefficient, b", is independent of temperature, and is fairly constant within an homologous series such as the PAQR polymers.

5. The Figure of Merit for piezo-resistivity of the polymers is greater than that of the existing metallic strain gages, suggesting their potential use as pressure-sensing devices.

6. The pressure-resistance measurements conducted with tellurium, were strongly affected by the p-type TeO_2 impurity present in the sample-giving a constant energy gap over the pressure range and a high initial thermoelectric-power coefficient, which decreased with increased pressure.

Appendix

Permeation Coefficient Calculation

$$\text{Leak rate} \leq 2.8 \times 10^{-4} \text{ mm/min.}$$

$$\text{Sample Thickness} = 10 \text{ mils} = 2.54 \times 10^{-2} \text{ cm}$$

$$\text{Permeation coefficient} = \frac{\text{cc/sec} \quad \text{(thickness)} \quad \text{cm}}{\text{area (cm)}^2 \quad \Delta P \quad \text{(atm)}} = P$$

$$\text{Volume of system} = V = 50 \text{ cc}$$

$$dV/dt = V/\text{st'd } P\ (dP/dt) = \frac{(2.8 \times 10^{-4}) \quad (50)}{(60) \qquad (760)}$$

$$dV/dt \leq 3.1 \times 10^{-7} \text{ cm}^3/\text{sec}$$

$$P = \frac{dV/dt \ (\text{Thick.})}{A \quad \Delta P} = \frac{(3.1 \times 10^{-7}) \ (2.54 \times 10^{-2})}{(1.0 \times 10^{-1}) \ (1)}$$

$$P = 8 \times 10^{-8} \ \frac{\text{cm}^3/\text{sec} - \text{cm}}{\text{cm}^2 - \text{atm}}$$

Figure of Merit Calculation

$$\text{FOM} = \frac{\left(\frac{\partial R}{\partial P}\right)_T \frac{\Delta P}{R}}{\left(\frac{\partial R}{\partial T}\right)_P \frac{\Delta T}{R} + \frac{\sum_i V_i}{(I_g R = V_g)}}$$

where R = resistance of pressure sensing element

P = pressure (atm)

ΔP = pressure increment (1 atm)

T = absolute temperature ($^\circ$K)

ΔT = absolute temperature increment (1°K)

$\sum_i \delta V_i$ = sum of all stray emf's which can affect galvanometer of the Wheatstone bridge containing R

I_g = effective current in galvanometer

$V_g = RI_g$ = working voltage across galvanometer

E.g. for a metallic strain gage

$\left(\frac{\partial R}{\partial P}\right)_T \frac{1}{R} = 0.4 \times 10^{-5}$ atm^{-1} (Bridgman's work on Cr)

$\left(\frac{\partial R}{\partial T}\right)_P \frac{1}{R} = 2 \times 10^{-4}$ deg^{-1} (measured on Baldwin Lima SR-4 gage at the Plastics Laboratory)

let $\sum_i \delta V_i = 10\ \mu V = 10^{-5}$ volts (thermal emf's usually noted)

and $V_g = 1$ mV $= 10^{-3}$ volts (usual operation full scale)

Then $(FOM)_{SG} = \frac{0.4 \times 10^{-5}}{2 \times 10^{-4} + 10^{-5}/10^{-3}} = 0.4 \times 10^{-3}$

E.g. for a semiconducting polymer, 52 EHE

$\left(\frac{\partial R}{\partial P}\right)_T \frac{1}{R} = 2.61 \times 10^{-5}$ atm^{-1}

$\left(\frac{\partial R}{\partial T}\right)_P \frac{1}{R} = 1.14 \times 10^{-2}$ deg^{-1}

let $\sum_i \delta V_i = 10\ \mu V = 10^{-3}$ volts

and $V_g = 10^{-3}$ volts

Then $(FOM)_{52} = \frac{2.61 \times 10^{-5}}{1.14 \times 10^{-2} + 10^{-5}/10^{-3}} = 1.22 \times 10^{-3}$

BIBLIOGRAPHY

1. Pohl, H.A., Rembaum, A., and Henry A., Jo. Am. Chem. Soc. 84, 2699-704 (1962) Effect of High Pressure on Some Organic Semiconducting Polymers

2. Balchan, A.S., and Drickamer, H.G.; Jo. Chem. Phys. 34, (1961) p.1948

3. Ioffe, A.F., Physics of Semiconductors, Academic Press (1960), p.380

4. Pohl, H.A., and Engelhardt, E.H., Synthesis and Characterization of Some Highly Conjugated Semiconducting Polymers, Plastics Laboratory Technical Report No. 64A Princeton University 1962

5. Kommandeur, Jr., and Hall, F.R., Journal of Chem. Phys, 34, (1961) p.129

6. Johnson, V,A., Progress in Semiconductors, Vol. I, Heywood & Co., (1956)

7. Horne, R.A. Journal Applied Physics, 30, 393 (1959)

8. Eley, D.D., Research (London) (1960) p.293

9. Engelhardt, E.H., Synthesis and Characterization of Some Highly Conjugated Semiconducting Polymers, Masters Thesis, May 1961, Princeton University

PRINCETON UNIVERSITY

Distribution List for Technical Reports

Contract No. DA-31-124-ARO(D)-21

1s. Lockheed Aircraft Corp.
Technical Information Center
3251 Hanover Street
Palo Alto, California (1)

2n. Commanding Officer
Office of Naval Res. Branch Ofc.
346 Broadway
New York 13, New York (1)

3n. Commanding Officer
Office of Naval Res. Branch Ofc.
1030 E. Green Street
Pasadena, 1, California (1)

4n. Commanding Officer
Office of Naval Res. Branch Office
Box 39 Navy No.100 Fleet P.O.
Fleet Post Office
New York, New York (7)

5n. Director, Naval Res. Lab.
Washington 25, D.C.
Attn: Technical Inform. Officer (6)
Chemistry Division (2)
Code 6110 (1)

6n. Chief of Naval Research
Department of the Navy
Washington 25, D.C.
Attn: Code 425 (2)

7n. DDR&E
Technical Library
Room 3C-128, The Pentagon
Washington 25, D. C. (1)

8n. Technical Director
Research & Engineering Div.
Office of the Quartermaster General
Department of the Army
Washington 25, D. C. (1)

9n. Research Director
Clothing & Organic Materials Div.
Quartermaster R&D
U.S. Army
Natick, Massachusetts (1)

10n. Air Force
Office of Scientific Res. (SRC-E)
Washington, 25, D.C.
(1)

11n. Commanding Officer
Diamond Ordnance Fuze Labs.
Washington 25, D.C.
Attn: Tech. Information Ofc.
Branch 012 (1)
Mr. M. Lipnick (1)

12n. Office, Chief of R&D
Department of the Army
Washington 25, D. C.
Attn: Physical Sciences Div.(1)

13n. Chief, Bureau of Ships
Department of the Navy
Washington 25, D. C.
Attn: Code 342C (2)

14n. Chief, Bur. of Naval Weapons
Department of the Navy
Washington 25, D.C.
Attn: Technical Library (3)
Code RRMA-3 (1)

15n. ASTIA
Document Service Center
Arlington Hall Station
Arlington 12, Virginia (10)

16n. Director of Research
USASRDL
Fort Monmouth, New Jersey(1)

17n. Naval Radiological Def. Lab.
San Francisco 24, California
Attn: Technical Library (1)

18n. Naval Ordnance Test Sta.
China Lake, California
Attn: Head, Chem. Div. (1)
Code 40 (1)
Code 50 (1)

19n. Commanding Officer
U.S. Army Research Office
Box CM, Duke Station
Durham, North Carolina
Attn: Scientific Synthesis Ofc. (1)

20n. Brookhaven National Lab.
Chemistry Division
Upton, New York (1)

21n. Atomic Energy Commission
Research Division
Chemistry Programs
Washington 25, D. C. (1)

22n. Atomic Energy Commission
Division of Techn. Inform. Extension
Post Office Box 62
Oak Ridge, Tennessee (1)

23n. U.S. Army Chem. R&D Labs.
Technical Library
Army Chemical Center, Maryland (1)

24n. Ofc. of Technical Services
Department of Commerce
Washington 25, D.C. (1)

25n. Commanding Officer
Naval Air Development Center
Johnsville, Pennsylvania
Attn: Dr. Howard R. Moore (1)

26n. Aeronautical Systems Div.
ASRCNP
Wright-Patterson, AFB, Ohio (1)

27n. Naval Powder Factory
Indian Head, Maryland
Attn: Mr. A. F. Johnson (1)

28n. Naval Electronics Lab.
San Diego, California (1)

29n. Naval Ordnance Laboratory
Silver Spring, Maryland
Attn: Dr. Albert Lightbody (1)

30n. Materials Laboratory
New York Naval Shipyard
Brooklyn, New York (1)

31n. Commander
Mare Island Naval Shipyard
Rubber Laboratory
Vallejo, California (1)

32n. Naval Air Experiment Sta.
Philadelphia Naval Shipyard
Philadelphia 12, Pa. (2)

33n. Dr. J. H. Faull, Jr.
72 Fresh Pond Lane
Cambridge, Mass. (1)

34n. Dr. B. Wunderlich
Department of Chemistry
Cornell University
Ithaca, New York (1)

35n. Dr. A. V. Tobolsky
Department of Chemistry
Princeton University
Princeton, New Jersey (1)

36n. Dr. W. Heller,
Department of Chemistry
Wayne State University
Detroit, Michigan (1)

37n. Dr. U. P. Strauss
Department of Chemistry (1)
Rutgers University, New Brunswick

38n. Dr. E. G. Rochow
Department of Chemistry
Harvard University
Cambridge 38, Massachusetts (1)

39n. Mr. H. D. Moran
Aircraft Industries Assoc.
7660 Beverly Boulevard
Los Angeles 36, Calif. (10)

40n. Dr. R. S. Stein
Department of Chemistry
University of Massachusetts
Amherst, Massachusetts (1)

41n. Mr. E. J. Kohn
Code 6110
Naval Research Laboratory
Washington 25, D. C. (1)

42n. Commanding Officer
Ordnance Materials Res. Office
Watertown Arsenal
Watertown 72, Mass. (1)

43n. Dr. Leo Mandelkern
National Bureau of Standards
Washington 25, D.C.
(1)

44n. Dr. G. Barth-Wehrenalp, Dir.
Inorganic Research Department
Pennsalt Chemicals Corporation
Post Office Box 4388
Philadelphia 18, Penna. (2)

45n. Dr. Marjorie Vold
Department of Chemistry
University of Southern Calif.
Los Angeles, California (1)

46n. Commanding Officer & Dir.
U.S. Naval Civil Engr. Lab.
Port Hueneme, Calif.
Attn: Chemistry Division (1)

47n. Dr. T. G. Fox
Mellon Institute
4400 Fifth Avenue
Pittsburgh 13, Penna. (1)

48n. Dr. Riley Schaeffer
Department of Chemistry
Indiana University
Bloomington, Indiana (1)

49n. Library
Textile Research Institute
P.O. Box 625
Princeton, New Jersey (1)

50n. Plastics Tech. Eval. Center
Picatinny Arsenal
Dover, New Jersey (1)

51s. Commanding Officer
Engineer R&D Labs.
Fort Belvoir, Virginia
Attn: Document Center (1)

52s. Commanding Officer
U.S. Army Signal R&D Lab.
Fort Monmouth, New Jersey
Attn: SIGRA/SL-ADT (1)

53s. Commanding Officer
U.S. Army Signal R&D Lab.
Fort Monmouth, New Jersey
Attn: SIGRA/SL-ADJ (1)
(File Unit No.3, ECR Dept.)

54s. Commanding Officer
U.S. Army Signal R&D Lab.
Fort Monmouth, New Jersey
Attn: SIGRA/SL-TN (For Transmittal to Accredited British & Canadian Government Representatives) (3)

55s. Commanding Officer
U.S. Army Signal Equip. Support Agcy. Fort Monmouth, N.J.
Attn: SIGMS/ADJ (1)

56s. Commanding Officer
U.S. Army Signal Equip Support Agcy. Fort Monmouth, N.J.
Attn: SIGMS-SDM (1)

57s. Commanding Officer
U.S. Army Signal R&D Lab.
Fort Monmouth, New Jersey
Attn: SIGFM/EL-P (1)

58s. Commander
Air Force Command & Control Div.
Air R&D Command, U.S. Air Force
L.G. Hanscomb Field
Bedford, Mass
Attn: CROTIR-2 (1)

59s. Commander
Rome Air Development Center
Air R&D Command
Griffiss AFB, New York
Attn: RCSSID (1)

60s. Commanding Officer
U.S. Army Signal R&D Labs.
Fort Monmouth, New Jersey
Attn: SIGRA/SL-PE (1)

61s. Commanding Officer
U.S. Army Signal R&D Labs.
Fort Monmouth, New Jersey
Attn: SIGRA/SL-PEM (1)

62s. Advisory Group on
Electronic Parts
Moore School Building
200 South 33rd Street
Philadelphia 4, Pa. (4)

63s. Commanding Officer
U.S. Army Electronics Research
& Development Laboratory
Attn: Technical Documents Center
Fort Monmouth, New Jersey (1)

64s. General Electric Company
Research Laboratory
P.O. Box 1088
Schenectady, New York
Attn: Dr. A. M. Bueche (1)

65s. Tech. Information Center
Lockheed Missiles & Space Div.
3251 Hanover Street
Palo Alto, California
Attn: Mr. W. A. Kozumplik (1)

66s. U.S. Army Signal Corp.
Liaison Office
Aeronautical Systems Division
Attn: ASDL-9
Wright-Patterson AFB, Ohio (2)

67s. USNSRD, Facilities
Clothing & Textile Division
3rd Avenue & 29th Street
Brooklyn 32, New York
Librarian (1)

68s. C.O. USASRDL
Fort Monmouth, New Jersey
Attn: SIGRA/SL-XE
Dr. H. H. Kedesdy (1)

69s. C. O. USASRDL
Fort Monmouth, New Jersey
Attn: SIGRA/SL-PDP
Dr. H. Mette (1)

70s. Chief, U.S. Security Agcy.
Arlington Hall Station
Arlington 12, Virginia (2)

71s. Deputy President, USA
Security Agency Board
Arlington Hall Station
Arlington 12, Virginia (1)

72s. Space Technology Labs.
P.O. Box 95001
Los Angeles 45, Calif. (1)

73s. Dr. M.S. Cohen, Chief
Propellants Synthesis Section
Reaction Motors Division
Denville, New Jersey (1)

74s. Boeing Airplane Co.
Transport Division
P.O. Box 707
Renton, Washington
Attn: Mr. F.N. Markey,
Unit Chief (1)

75s. Commanding Officer
Ordnance Materials Res. Ofc.
Watertown Arsenal
Watertown 72, Mass.
Attn: RPD (1)

76s. Commanding Officer
Rock Island Arsenal
Rock Island, Illinois
Attn: Mr. R. Shaw, Laboratory(1)

77s. Monsanto Chemical Co.
Research & Engineering Div.
Boston 49, Massachusetts
Attn: Mr. K. Warren Easley (1)

78s. R. R. Sowell,
Dept. 1110, Sandia Corp.
Albuquerque, New Mexico (1)

79s. L. M. Berry,
Organ. 8115, Sandia Corp.
Livermore, California (1)

80.s. Commanding Officer
U.S. Army Electronics Research &
Development Laboratory
Attn: Director of Research
Fort Monmouth, New Jersey (1)

81. s.
Commanding Officer
U.S. Army Electronics Research &
Development Laboratory
Attn: SELRA-PEE (Mr. E. Beekman)
Fort Monmouth, New Jersey (1)

82.s. Mr. A. J. Quant
Organization 1110
Sandia Corporation
Albuquerque, New Mexico (1)

83.s. Mr. J. E. Hansen
Thiokol Chemical Corp.
Wasatch Div.
Brigham City, Utah (1)

84. s.
U.S. Army Research Office (Durham)
Box CM, Duke Station
Durham, North Carolina (25)

85.n.
Code 6120
Naval Research Laboratory
Washington 25, D. C.
Attn: Dr. R. B. Fox (1)
Mr. J. E. Cowling (1)
Dr. A. L. Alexander (1)
Dr. D. L. Venezky (1)

86.n.
Mr. J. A. Kies (1)
Code 6210
Naval Research Laboratory
Washington 25, D. C.